NACA TN 2251

NATIONAL ADVISORY COMMITTEE FOR AERONAUTICS

TECHNICAL NOTE 2251

EFFECTS OF MACH NUMBER UP TO 0.34 AND REYNOLDS NUMBER UP TO 8×10^6 ON THE MAXIMUM LIFT COEFFICIENT OF A WING OF NACA 66-SERIES AIRFOIL SECTIONS

By G. Chester Furlong and James E. Fitzpatrick

Langley Aeronautical Laboratory
Langley Field, Va.

Washington
December 1950

NATIONAL ADVISORY COMMITTEE FOR AERONAUTICS

TECHNICAL NOTE 2251

EFFECTS OF MACH NUMBER UP TO 0.34 AND REYNOLDS NUMBER UP TO 8×10^6 ON THE MAXIMUM LIFT COEFFICIENT OF A WING OF NACA 66-SERIES AIRFOIL SECTIONS

By G. Chester Furlong and James E. Fitzpatrick

SUMMARY

The effects of Mach number and Reynolds number on the maximum lift coefficient of a wing of NACA 66-series airfoil sections are presented. The wing was tested through the speed range of the Langley 19-foot pressure tunnel at two tunnel pressures. The ranges of Mach number obtained at the two tunnel pressures were 0.10 to 0.34 and 0.07 to 0.26; the corresponding Reynolds number ranges were from 1.36×10^6 to 4.66×10^6 and from 2.20×10^6 to 8.00×10^6, respectively.

The wing was tested with full-span and partial-span split flaps deflected 60° and without flaps. Chordwise-pressure-distribution measurements were made for all flap configurations of the model.

For a given value of Mach number the values of maximum lift coefficient were increased when the Reynolds number was increased. For a given value of Reynolds number an increase in Mach number in the subcritical range caused small reductions in maximum lift coefficient; whereas an increase in Mach number that caused the critical speed to be exceeded resulted in large reductions in maximum lift coefficient. These effects resulted in peak values of maximum lift coefficients being obtained at free-stream Mach numbers of approximately 0.212 and 0.227 for the plain wing and 0.138 and 0.196 for the full-span flaps-deflected configuration, depending on the Reynolds number range involved. Although an increase in Mach number and Reynolds number may produce several types of variations of maximum lift coefficient with Reynolds number, the peak values of maximum lift coefficient on the present wing appeared to occur with the attainment of sonic speed locally on the wing. Sonic speed was measured coincident with the peak value of maximum lift coefficient for only one configuration; however, indications were that, with the available leading-edge orifices, the minimum pressures were not measured in all cases.

Roughness on the leading edge materially reduced the effect of Reynolds number on maximum lift coefficient, but Mach number effects

in the subcritical speed range were of the same order as those obtained with the smooth wing.

INTRODUCTION

The influence of Reynolds number on the maximum lift coefficient and stall phenomenon has received both qualitative and quantitative treatment in references 1 and 2. Subsequent investigations reported in references 3 and 4 have indicated that serious compressibility effects can be encountered at Mach numbers in the landing-speed range of present-day airplanes. Thus, a knowledge of the interrelated effects of Mach number and Reynolds number on maximum lift coefficient is significant not only in flight problems concerning airplane maneuvering performance but also in the interpretation of low-speed wind-tunnel data. A study has been initiated, therefore, to explain at least qualitatively the isolated and combined influences of Mach number and Reynolds number on maximum lift coefficient.

The study is being conducted in the Langley 19-foot pressure tunnel and in the Langley 16-foot high-speed tunnel. The tests in the Langley 19-foot pressure tunnel are concerned with the interrelated effects of Mach number and Reynolds number on the low-speed (Mach numbers below 0.350) maximum lift. The tests in the Langley 16-foot high-speed tunnel are principally concerned with the effects of Mach number on maximum lift at Mach numbers up to 0.650. One wing which incorporates NACA 230-series airfoil sections has been tested in both tunnels, and the results obtained are contained in references 5 and 6. Another wing, having the same plan form as the first but incorporating NACA 66-series airfoil sections, has been tested in the Langley 16-foot high-speed tunnel, and the results are presented in references 7 and 8.

The present paper contains the results of an investigation made with the wing of NACA 66-series airfoil sections in the Langley 19-foot pressure tunnel. The tests were conducted at tunnel pressures of 14.7 and 33 pounds per square inch absolute. These tunnel pressures allowed Mach number ranges from 0.100 to 0.340 and from 0.070 to 0.260 to be obtained. The corresponding Reynolds number ranges were from 1.36×10^6 to 4.66×10^6 and from 2.20×10^6 to 8.00×10^6, respectively. The investigation included force tests and chordwise-pressure-distribution measurements at six spanwise stations. The tests were made with the wing model both without flaps and with full-span and partial-span split flaps deflected 60°. In addition, leading-edge-roughness tests were made with the plain wing and with partial-span flaps deflected.

SYMBOLS

C_L	lift coefficient (Lift/$q_o S$)
$C_{L_{max}}$	maximum lift coefficient
$c_{l_{max}}$	two-dimensional maximum lift coefficient
M_o	free-stream Mach number (V_o/a)
M_l	local Mach number at a point on wing
P	pressure coefficient $\left(\frac{p - p_o}{q_o}\right)$
P_{min}	minimum pressure coefficient on wing measured at $C_{L_{max}}$
R_o	free-stream Reynolds number ($\rho V_o \bar{c}/\mu$)
$\bar{c}$	mean aerodynamic chord, feet $\left(\frac{2}{S}\int_0^{b/2} c^2 dy\right)$
a_c	lift-curve slope measured from data
a_i	lift-curve slope converted to incompressible-flow condition (see reference 9)
C	cross-sectional area of test section, square feet
D	diameter of tunnel test section, feet
S	wing area, square feet
V_o	free-stream velocity, feet per second
a	speed of sound, feet per second
s	distance, measured along surface, from leading edge to center of orifice
b	wing span, feet
c	local chord, feet
p	local static pressure, pounds per square foot
p_o	free-stream static pressure, pounds per square foot

q_o	free-stream dynamic pressure, pounds per square foot
x	distance parallel to chord from leading edge (chord parallel to plane of symmetry), feet
y	lateral distance perpendicular to plane of symmetry, feet
α	angle of attack of wing root chord, degrees
α_{max}	angle of attack at maximum lift, degrees
δ_w	jet-boundary correction factor (see reference 10)
ρ	mass density of air, slugs per cubic foot
μ	coefficient of viscosity of air, slugs per foot-second

MODEL, APPARATUS, AND TESTS

Model and Apparatus

The plan form of the wing and principal dimensions are shown in figure 1. The wing has a span of 12 feet, an aspect ratio of 6, and a washout of 1.5°. The wing is constructed of solid steel and is believed to be rigid enough to avoid appreciable amounts of deflection during the tests. The tips are semielliptical in cross section and begin at the 99-percent-semispan station.

The airfoil section at the plane of symmetry was the NACA 66(215)-116 (a = 0.6) except for a slight reduction of 0.1 percent chord in the leading-edge radius. The same was true for the construction tip which was the NACA 66(215)-216 (a = 0.6) airfoil. This slight difference is not believed to affect either the qualitative or the quantitative results presented herein.

The installation and geometry of the 55- and 99-percent-span 20-percent-chord split flaps are shown in figure 1. The flaps were deflected 60° to the lower surface.

Leading-edge roughness was obtained for some of the tests by applying No. 60 (0.011-in. mesh) carborundum grains to a thin layer of shellac across the complete span on both upper and lower surfaces for a surface length of 8 percent chord measured from the leading edge. The grains covered 5 to 10 percent of the affected area.

The model was mounted on the normal wing-support system of the Langley 19-foot pressure tunnel. (See fig. 2.) The aerodynamic forces and moments were measured by a simultaneous-recording six-component balance system.

The wing contained approximately 35 surface-pressure orifices at each of six spanwise stations. The location of the orifice stations are shown in figure 1, and the chordwise distribution of pressure orficies are listed in table I. The original pressure leads were conducted internally to a pipe protruding from the trailing edge at the wing root (fig. 1). The pressure leads were then brought to multiple-tube manometers through a specially designed tube-transfer system. This system, shown in figure 3, allowed continuous testing through the angle-of-attack range without necessitating manual adjustments. Although the boom was counterbalanced, it did not allow reliable force tests to be made simultaneously with pressure measurements; consequently, force tests were made with the tube-transfer system removed. During the force tests a short fairing cap covered the pipe extending from the trailing edge at the plane of symmetry (fig. 2).

The original leading-edge orifice distribution as given in reference 7 was found to be insufficient to define either the position or the magnitude of the minimum pressure. Extra orifices were consequently installed in the wing between the leading-edge orifice and the orifice immediately behind it in order to measure the peak minimum pressure as closely as feasible. The additional pressure leads were conducted along the lower surface and down the support strut to the multiple-tube manometer. The extra orifice leads were brought out sufficiently far behind the leading edge on the lower surface to make possible interference with the minimum peak measurement on the upper surface negligible.

Tests

Tests were conducted at two tunnel pressures of 14.7 and 33 pounds per square inch absolute. The ranges of Mach number and Reynolds number thus obtained were as follows:

Tunnel pressure (lb/sq in. abs.)	Mach number range	Reynolds number range
14.7	0.100 to 0.340	1.36×10^6 to 4.66×10^6
33	.070 to .260	2.20×10^6 to 8.00×10^6

Force tests with the wing smooth were made through the speed range at both tunnel pressures for the model equipped with full-span and partial-span flaps and without flaps. Force tests with leading-edge

roughness were made for the model equipped with partial-span flaps and without flaps through the speed range at both tunnel pressures.

With the exception of the full-span flap configuration, pressure-distribution tests were made at both tunnel pressures for the same values of Mach number and Reynolds number obtained in the force tests. Some pressure-distribution tests with leading-edge roughness were made on the wing without flaps.

The wing was tested through an angle-of-attack range from -6.5° through the stall.

CORRECTIONS TO DATA

Force Tests

The lift coefficients have been corrected for support-strut tare and interference as determined by tare tests with an image support system.

The angles of attack have been corrected for air-stream misalinement and jet-boundary effects. The air-stream misalinement was determined during the tare tests. The jet-boundary correction was determined by the following equation derived from reference 10:

$$\Delta\alpha = \left(1 + \frac{1.05\bar{c}}{D\sqrt{1 - M_o^2}}\right)\delta_w \frac{S}{C}\, 57.3 C_L$$

This equation contains the angle-of-attack correction at the lifting line for the case of a wing with an elliptical spanwise load distribution and also an additional correction for the induced streamline curvature. The term $\sqrt{1 - M_o^2}$ has been introduced to account for compressibility effects (reference 9). For the tests in the Langley 19-foot pressure tunnel, the correction to the angle of attack became $0.678 C_L$.

Pressure-Distribution Tests

No corrections have been applied to the local values of static pressure. The orifice stations were selected so that the local effects of the struts and walls on these pressures could be assumed negligible. In the computation of the pressure coefficients, however, average dynamic pressure and average static pressure across the span have been used inasmuch as tunnel surveys indicate these pressures to be constant within 1.5 percent of the free-stream dynamic pressure over the survey stations.

RESULTS

The variations of Mach number with Reynolds number obtained through the speed range of the Langley 19-foot pressure tunnel at the two tunnel pressures and the Langley 16-foot high-speed tunnel are presented in figure 4. For a given value of Reynolds number, the maximum deviation in Mach number for a particular tunnel pressure is approximately 0.015.

As the tests of the wing proceeded at atmospheric pressure, it was found that the maximum-lift and minimum-pressure-coefficient data could not be repeated in the speed range at which the minimum pressure coefficients were approaching the critical (M_l = 1.000). The disagreement between supposedly identical tests was approximately 1.5° for the angle of attack of maximum lift and 2.6 for the minimum pressure coefficient (approx. 18 percent of the minimum pressure coefficient recorded). The supposition was advanced that variations in the amount of condensation might be the responsible factor. From consideration of the dew point and stagnation temperature, it was established that the air conditions could have resulted in condensation. In order to remove this possibility, the tunnel was sealed and the tests were repeated at a relationship between dew point and stagnation temperature which unpublished data based on nuclei-formation theory (Lewis Laboratory) indicated to be in the condensation-free region. Under these dry-air conditions it was possible to repeat more closely both the lift and pressure data. All the data presented in the present paper, therefore, were obtained with the air conditions in the tunnel such as to insure condensation-free flow.

The basic lift data obtained in the Langley 19-foot pressure tunnel are presented in figures 5 to 7 for the plain wing and for the wing with partial-span and full-span flaps deflected, respectively. (The abscissa scale is staggered and the zero axis for each curve is identified by the test-point symbol associated with the curve.) For some test conditions of the plain wing and partial-span flap configuration, data were also obtained with leading-edge roughness.

The slopes of the lift curves obtained in both the Langley 19-foot pressure tunnel and the Langley 16-foot high-speed tunnel and corrected to incompressible-flow conditions by the method of reference 9 have been plotted against Mach number in figure 8. Inasmuch as Reynolds number has a negligible effect on lift-curve slope, the results presented in figure 8 indicate the applicability of the method presented in reference 9 for converting slopes measured in incompressible flow to compressible-flow conditions.

The maximum lift coefficients and corresponding angles of attack have been plotted against both Mach number and Reynolds number in figure 9 for the plain wing and the partial-span and full-span flap configurations. Similar data for the plain wing and partial-span flap configuration with leading-edge roughness are presented in figure 10. The variations of maximum lift coefficient with Mach number and Reynolds number obtained in the Langley 19-foot pressure tunnel for all model configurations and tunnel conditions resemble those presented in references 3, 5, and 6. The value of maximum lift coefficient, for example, increases with an increase in airspeed to a maximum or peak value, after which the maximum lift coefficient decreases with a further increase in airspeed. The variations of maximum lift with Mach number and Reynolds number for the configurations with leading-edge roughness (fig. 10) are rather small. Both the maximum lift and angle of attack for maximum lift tend to drop slightly in the high Mach number and Reynolds number ranges, and this tendency is more noticeable in the case of angle of attack for maximum lift.

The variations of minimum pressure coefficients with both Mach number and Reynolds number for the configurations tested in the Langley 19-foot pressure tunnel are included in figure 9. The minimum pressure coefficients were measured at $\frac{x}{c} = 0.0018$, station 2, for all model configurations and at both tunnel pressures. Similar data from the Langley 16-foot high-speed tunnel (references 7 and 8) are not comparable because, as previously mentioned, the original orifice distribution was insufficient to determine the minimum pressure coefficient.

Tuft studies of the flow separation on the wing are presented in figure 11. Representative chordwise-pressure-distribution data have been presented in figure 12 to illustrate the differences in stalling characteristics obtained at different airspeeds.

Chordwise pressure distributions obtained with and without leading-edge roughness on the retracted flap configuration are compared in figure 13.

Variations of local Mach number with free-stream Mach number and with distance on the surface from the leading edge are presented in figures 14 and 15, respectively, for the wing with and without partial-span flaps and at the two tunnel pressures. The local Mach numbers were computed from the pressure coefficients obtained at station 2 on the wing.

DISCUSSION

Reynolds Number Effects

NACA 6-series airfoil sections are characterized by separation of the laminar boundary layer near the leading edge at low Mach and Reynolds numbers when the low-drag range is exceeded (reference 11). Several investigations have shown that the boundary-layer flow thus produced will reattach itself to the airfoil surface downstream of the separation point as a turbulent boundary layer at a Reynolds number dependent primarily on airfoil thickness (reference 12). The enclosed region of separated flow is commonly known as a separation bubble.

Reynolds number has a negligible effect on the maximum lift coefficient below the Reynolds number at which a separation bubble forms. Increase in Reynolds number will diminish the size of the bubble, and the following two effects are noted: the point of reattachment of the bubble moves forward, and the turbulent boundary layer over the rear part of the airfoil becomes more resistant to separation (reference 12) and, therefore, higher angles of attack and accompanying increases in maximum lift coefficient are obtained before the flow breaks down. When the bubble is finally eliminated, and the transition point has moved to the position of minimum pressure, as pointed out in reference 1, the maximum lift coefficient will not increase with a further increase in Reynolds number.

The presence of a separation bubble on the NACA 66-series wing through the Reynolds number range of the present tests (1.36×10^6 to 8.00×10^6) would be expected on the basis of the data presented in reference 12. Lampblack studies (not photographically recorded) were made on the present wing at a Reynolds number of 1.38×10^6 (corresponding Mach number 0.100) which gave experimental evidence of the separation bubble. The increases in maximum lift coefficient obtained by increasing the Reynolds number at a given Mach number also give an indirect indication of the separation bubble. For example, at a Mach number of 0.100, increasing the tunnel pressure to 33 pounds per square inch increased the Reynolds number from 1.50×10^6 to 3.15×10^6 and the maximum lift coefficient of the plain wing from 0.97 to 1.30 (fig. 9(a)).

In order to indicate the variation of maximum lift coefficient with Reynolds number that would be expected through the Reynolds number range of the present tests, but through a lower Mach number range, the results obtained in two-dimensional tests of NACA 66-series airfoils similar to those of the present wing are presented in figure 16. The airfoil with camber shows an increase in maximum lift coefficient between a Reynolds number range of 3.00×10^6 and 6.00×10^6 and a slight decrease in maximum lift coefficient between a Reynolds number range of 6.00×10^6

and 9.00×10^6. If it had been possible to obtain the variation in Reynolds number of the present tests with the same increase in Mach number, the NACA 66-series wing would probably exhibit similar maximum lift characteristics. It should be pointed out that the two-dimensional data were obtained through a corresponding Mach number range from 0.110 to 0.161 and, therefore, in the higher Reynolds number range the lack of any beneficial Reynolds number effect may be due in part to adverse Mach number effects.

At atmospheric pressure the maximum lift coefficient of the plain wing increased with an increase in Reynolds number up to a Reynolds number of 3.30×10^6 ($M_o = 0.227$) and then decreased rather abruptly through the remainder of the Reynolds number range (fig. 9(a)). Inasmuch as the maximum lift coefficient would be expected to increase through the entire Reynolds number range of the atmospheric pressure tests, the loss in maximum lift coefficient which begins at $M_o = 0.227$ is associated with the occurrence of local Mach numbers near unity. This effect is subsequently discussed. For the partial-span and full-span flap configurations, the maximum lift coefficients increased up to Reynolds numbers of of 2.90×10^6 ($M_o = 0.196$) and 2.75×10^6 ($M_o = 0.191$), respectively, and decreased abruptly through the remainder of the Reynolds number range. At tunnel pressures of 33 pounds per square inch the maximum lift coefficient of the plain wing increased with an increase in Reynolds number up to a Reynolds number of about 5.50×10^6 and then leveled off and began decreasing at a Reynolds number of about 6.50×10^6 ($M_o = 0.212$) For the partial-span and full-span flap configurations, the maximum lift coefficients increased up to Reynolds numbers of 6.05×10^6 ($M_o = 0.194$) and 4.50×10^6 ($M_o = 0.138$), respectively, and decreased abruptly through the remainder of the Reynolds number range. The decreases in maximum lift coefficient are again associated with the critical speed of the wing and, because of the increase in Reynolds number, the decrease in maximum lift coefficient occurs at a lower stream Mach number than in the atmospheric-pressure tests.

The general trends of the results obtained with partial-span and full-span flaps are similar to those obtained on the plain wing.

Mach Number Effects

The effects of Mach number on the maximum lift coefficient of airfoils have not been isolated and studied as thoroughly as the effects of Reynolds number.

The results of the tests in reference 5 indicate that at a given value of Reynolds number an increase in Mach number caused a moderate decrease in the maximum lift coefficient even though the local velocities on the surface of the wing were somewhat below sonic speed. At least a

part of this decrease in maximum lift coefficient can be attributed to the fact that the adverse pressure gradients become more severe as the Mach number is increased. The possiblity is suggested that Mach number also influences the flow characteristics within the separation bubble.

When the Mach number is such that sonic speed is reached locally on the wing, the disturbance causes a flow breakdown, and the losses in maximum lift become much greater than those obtained in the subcritical speed range. Inasmuch as the critical pressures (sonic speed) are reached at progressively lower angles of attack in this Mach number range (Reynolds number constant), the losses in maximum lift coefficient become even greater (reference 5). In this Mach number range (sonic speed exceeded on the wing) the influence of Reynolds number is seen to be reduced markedly; in fact, as shown in reference 13 in the Mach number range above 0.500, the effects of Reynolds number on the maximum lift coefficient were negligible.

The decreases in maximum lift coefficient obtained by decreasing the tunnel pressure (increasing Mach number at a given Reynolds number) give a measure of the magnitude of the loss to be expected. For example, in the subcritical Mach number range, at a Reynolds number of 2.50×10^6 decreasing the tunnel pressure to atmospheric pressure increased the Mach number from 0.080 to 0.180 and decreased the maximum lift coefficient of the plain wing from 1.21 to 1.14 (fig. 9(a)). In the supercritical Mach number range (Reynolds number 4.50×10^6), decreasing the tunnel pressure to atmospheric pressure increased the Mach number from 0.145 to 0.328 and decreased the maximum lift coefficient of the plain wing from 1.41 to 1.04 (fig. 9(a)).

Interrelated Effects of Mach and Reynolds Number

The data of the present investigation and the data presented in reference 5 indicate that at a given Reynolds number an increase in Mach number causes a decrease in maximum lift coefficient, and if the increase in Mach number causes the critical speed (sonic) to be exceeded, the decrease in maximum lift coefficient becomes very large. As Mach number and Reynolds number increase, therefore, the isolated effects may be expected to produce variations of maximum lift coefficient peculiar to a particular wing. Before proceeding into a discussion of the interrelated effects of Mach number and Reynolds number on the maximum lift coefficient of the present NACA 66-series wing, it appears desirable to consider qualitatively some of the general aspects of both the isolated and interrelated effects.

Case I.- Consider a wing in which the taper ratio and twist are such as to promote a very rapid stall progression. Furthermore, assume that the airfoil sections incorporated in this wing will show large

increases in maximum lift with increases in Reynolds number obtained without increasing the Mach number (fig. 17(a)). With the airspeed held constant at a very low value, compressibility effects can be assumed negligible. For the flight case or in the normal wind-tunnel testing procedure, however, the increase in Reynolds number is usually obtained by increasing the airspeed and, therefore, the Mach number is also increasing. (For example, see fig. 4.) If the Mach number is increasing with Reynolds number, the maximum lift coefficient will not increase as greatly as it did when compressibility effects could be neglected. The increase in Mach number may, within the Reynolds number range considered, cause the surface velocities to reach sonic speed. If sonic speed is reached locally on the wing and the airspeed is further increased (M_O and R_O increasing), substantial losses in maximum lift coefficient will be obtained. Variations of maximum lift coefficient with Reynolds number for the cases of $M_O = 0$ and of M_O increasing with R_O are shown schematically in figure 17(a). Under the assumed conditions the maximum lift coefficient would increase with an increase in Mach number and Reynolds number until the critical speed (sonic) was reached on the wing surface. The maximum lift coefficient would then decrease with a further increase in Mach number and Reynolds number. The data obtained on the NACA 230-series wing illustrate these effects (reference 5).

Case II.- Some wings employ airfoil sections which show only small variations in maximum lift coefficient with Reynolds number (for the condition where compressibility effects can be assumed negligible). The effect of increasing the Mach number when the Reynolds number is increased (airspeed increasing) are the same as in case I; however, the variation of maximum lift coefficient with Reynolds number (shown schematically in fig. 17(b)) does not possess a peak value of maximum lift coefficient that is coincident, as in case I, with the attainment of sonic speed. The highest value of maximum lift coefficient under the assumed conditions would occur at the lowest value of Mach number and Reynolds number.

Case III.- If twist and taper ratio are employed in such a way as to make the wing of case I have a very gradual stall progression, the wing will have a variation of maximum lift coefficient with Reynolds number shown schematically for case III in figure 17(c). When sonic speed is attained by the surface velocities, the disturbance may be so localized that, although the rate of increase of maximum lift coefficient is greatly decreased, the maximum lift coefficient is not reduced until sonic speed has been reached over a great part of the wing.

Mixed cases.- The foregoing cases were idealized, and it should be recognized that any particular wing may actually possess, through a given Reynolds number range, the maximum lift characteristics of cases I and II and, to a degree, the stalling characteristics of case III. For example, through the Reynolds number range from 2.00×10^6 to 8.00×10^6 the maximum lift coefficient may increase greatly between Reynolds numbers

of 2.00×10^6 and 6.00×10^6 and then remain effectively constant between Reynolds numbers of 6.00×10^6 and 8.00×10^6. If the corresponding Mach number range causes sonic speed to be reached on the wing between Reynolds numbers of 2.00×10^6 and 6.00×10^6, the highest value of maximum lift coefficient would probably be coincident with the attainment of sonic speed unless the conditions of case III applied. If the Mach number range caused sonic speed to be reached between Reynolds numbers of 6.00×10^6 and 8.00×10^6, the highest value of maximum lift coefficient would be measured prior to the attainment of sonic speed.

Correlation between minimum pressure coefficient and peak maximum lift coefficients.- The critical pressure coefficient was measured coincident with the decrease in maximum lift coefficient for only the partial-span flap configuration (tunnel pressure, 33 lb/sq in.). Pressure coefficients which correspond to local Mach numbers of 0.850 to 0.900 were measured coincident with the decrease in maximum lift coefficient for the other model and tunnel conditions. It is conjectured, however, that as in cases I and II the critical pressure coefficient was reached locally on the wing before any appreciable losses in maximum lift coefficient were encountered.

Although additional orifices were installed in the leading edge of the wing during the present tests, the chordwise and spanwise spacing of the orifices, the Mach number gradients which existed over the orifices themselves, and the ability of a liquid manometer to average accurately a fluctuating pressure did not necessarily give measurements of the minimum pressures. For example, the variations of local Mach number with free-stream Mach number (fig. 14) indicate that, for the wing with and without partial-span flaps at a tunnel pressure of 33 pounds per square inch, sonic speed was measured at a free-stream Mach number very close to that at which the peak value of maximum lift coefficient was attained. At a tunnel pressure of 14.7 pounds per square inch, however, the data for both configurations indicate a greater difference between the free-stream Mach numbers at which the critical pressure coefficient and the peak maximum lift coefficient were measured. All minimum-pressure-coefficient data were obtained at the same orifice $\left(\frac{x}{c} = 0.0018, \text{ station 2, table I}\right)$; however, changes in model configuration and tunnel pressure (changes in Reynolds number) might be expected to cause chordwise and spanwise changes in the location of the minimum pressure. For each variation of local Mach number with free-stream Mach number an inflection occurs in the vicinity of sonic speed. In the case of the partial-span-flaps configuration, the inflection occurs with the attainment of sonic speed. For the same configuration the results obtained at an orifice located ahead of the orifice at which the minimum pressure coefficients were measured indicate that the inflection is obtained before sonic speed; therefore, the variation of local Mach number with free-stream Mach number is similar to that obtained for the other model configuration and tunnel pressures. The variations of local Mach number with distance from the

leading edge (fig. 15) illustrate the extremely large Mach number gradients encountered in the present tests. The data seem to indicate that the Mach numbers for peak maximum lift coefficient are more closely defined in the tests made at 33 pounds per square inch than in the tests made at 14.7 pounds per square inch.

Wing with Leading-Edge Roughness

The results obtained with leading-edge roughness indicate that $C_{L_{max}}$ was influenced by variations in M_o as well as by variations in R_o (fig. 10). The data indicate that in the Reynolds number range prior to the peak value of maximum lift the effect of Mach number for the configurations with leading-edge roughness was the same as for the smooth retracted-flaps configuration and approximately the same as for the partial-span flap configuration. For example, at a Reynolds number of 3.10×10^6 an increase in Mach number from 0.100 to 0.218 reduced the maximum lift coefficient by 0.07 for the rough and smooth plain-wing configuration. The increased pressure recovery required by the increase in Mach number probably is the cause for the similar effects of Mach number on the smooth and rough wing in the subcritical speed range. The pressure-distribution data presented in figure 13 indicate an appreciable reduction in the leading-edge pressures so that critical pressure coefficients were not obtained in the speed range of the present tests. No similarity between Mach number effects on the smooth- and rough-wing conditions is therefore evident after the critical pressure coefficients have been reached on the smooth-wing configurations. The maximum-lift-coefficient data (fig. 10) indicate an appreciable decrease in Reynolds number effect due to leading-edge roughness, and this decrease becomes even greater as the Mach number is increased. At a Mach number of 0.100, an increase in Reynolds number from 1.45×10^6 to 3.15×10^6 increased the maximum lift coefficient of the smooth flaps-retracted configuration by 0.33 and only by 0.09 after leading-edge roughness was applied. The reduction in Reynolds number effect on maximum lift coefficient at this Mach number is in relative agreement with that found on NACA 6-series airfoils in two-dimensional tests (reference 14).

SUMMARY OF RESULTS

The following remarks summarize the results obtained from an investigation made in the Langley 19-foot pressure tunnel at tunnel pressures of 14.7 and 33 pounds per square inch absolute to determine the effects of Mach number up to 0.34 and Reynolds number up to 8×10^6 on the maximum lift coefficient of a wing of NACA 66-series airfoil sections.

For a given value of Mach number the values of maximum lift coefficient were increased when the Reynolds number was increased. For a given value of Reynolds number an increase in Mach number in the subcritical speed range caused small reductions in maximum lift coefficient; whereas an increase in Mach number that caused the critical speed to be exceeded resulted in large reductions in maximum lift coefficients. These effects resulted in peak values of maximum lift coefficients being obtained at free-stream Mach numbers of approximately 0.212 and 0.227 for the plain wing and 0.138 and 0.196 for the full-span flaps-deflected configuration, depending on the Reynolds number range involved. Although an increase in Mach number and Reynolds number may produce several types of variations of maximum lift coefficient with Reynolds number, the peak values of maximum lift coefficient on the present wing appeared to occur with the attainment of sonic speed locally on the wing. Sonic speed was measured coincident with the peak value of maximum lift coefficient for only one configuration; however, indications were that, with the available leading-edge orifices, the minimum pressures were not measured in all cases.

Roughness on the leading edge materially reduced the effect of Reynolds number on maximum lift coefficient, but Mach number effects in the subcritical speed range were of the same order as those obtained with the smooth wing.

Some evidence indicated the possibility of losses in maximum lift due to condensation in the speed range where sonic speeds were approached on the wing.

Langley Aeronautical Laboratory
National Advisory Committee for Aeronautics
Langley Field, Va., September 7, 1950

REFERENCES

1. Jacobs, Eastman N., and Sherman, Albert: Airfoil Section Characteristics as Affected by Variations of the Reynolds Number. NACA Rep. 586, 1937.

2. Pinkerton, Robert M.: The Variation with Reynolds Number of Pressure Distribution over an Airfoil Section. NACA Rep. 613, 1938.

3. Muse, Thomas C.: Some Effects of Reynolds and Mach Numbers on the Lift of an NACA 0012 Rectangular Wing in the NACA 19-Foot Pressure Tunnel. NACA CB 3E29, 1943.

4. Stack, John, Fedziuk, Henry A., and Cleary, Harold E.: Preliminary Investigation of the Effect of Compressibility on the Maximum Lift Coefficient. NACA ACR, Feb. 1943.

5. Furlong, G. Chester, and Fitzpatrick, James E.: Effects of Mach Number and Reynolds Number on the Maximum Lift Coefficient of a Wing of NACA 230-Series Airfoil Sections. NACA TN 1299, 1947.

6. Pearson, E.O., Jr., Evans, A. J., and West, F. E., Jr.: Effects of Compressibility on the Maximum Lift Characteristics and Spanwise Load Distribution of a 12-Foot-Span Fighter-Type Wing of NACA 230-Series Airfoil Sections. NACA ACR L5G10, 1945.

7. Cooper, Morton, and Korycinski, Peter F.: The Effects of Compressibility on the Lift, Pressure, and Load Characteristics of a Tapered Wing of NACA 66-Series Airfoil Sections. NACA TN 1697, 1948.

8. West, F. E., Jr., and Hallissy, J. M., Jr.: The Effects of Compressibility on the Normal-Force, Pressure, and Load Characteristics of a Tapered Wing of NACA 66-Series Airfoil Sections with Split Flaps. NACA TN 1759, 1948.

9. Goldstein, S., and Young, A. D.: The Linear Perturbation Theory of Compressible Flow with Application to Wind-Tunnel Interference. R. & M. No. 1909, British A.R.C., 1943.

10. Silverstein, Abe, and White, James A.: Wind-Tunnel Interference with Particular Reference to Off-Center Positions of the Wing and to the Downwash at the Tail. NACA Rep. 547, 1935.

11. Von Doenhoff, Albert E., and Tetervin, Neal: Investigation of the Variation of Lift Coefficient with Reynolds Number at a Moderate Angle of Attack on a Low-Drag Airfoil. NACA CB, Nov. 1942.

12. Loftin, Laurence K., Jr., and Bursnall, William J.: The Effects of Variations in Reynolds Number between 3.0×10^6 and 25.0×10^6 upon the Aerodynamic Characteristics of a Number of NACA 6-Series Airfoil Sections. NACA TN 1773, 1948.

13. Spreiter, John R., and Steffen, Paul J.: Effect of Mach and Reynolds Numbers on Maximum Lift Coefficient. NACA TN 1044, 1946.

14. Loftin, Laurence K., Jr., and Smith, Hamilton A: Aerodynamic Characteristics of 15 NACA Airfoil Sections at Seven Reynolds Numbers from 0.7×10^6 to 9.0×10^6. NACA TN 1945, 1949.

15. Abbott, Ira H., Von Doenhoff, Albert E., and Stivers, Louis S., Jr.: Summary of Airfoil Data. NACA Rep. 824, 1945.

TABLE I.- ORIFICE LOCATIONS

x/c		x/c		x/c	
Upper	Lower	Upper	Lower	Upper	Lower
Station 1		Station 2		Station 3	
0	-----	0	-----	0	-----
------	-----	.0004	-----	.0009	-----
.0015	-----	.0018	-----	.0010	-----
------	-----	.0019	-----	.0068	-----
.013	0.013	.013	0.013	.013	0.013
.038	.038	.038	.038	.038	.038
.063	.063	.063	.063	.063	.063
.125	.088	.125	.088	.125	.088
.175	.125	.175	.125	.175	.125
.225	.175	.225	.175	.225	.175
.275	.250	.275	.250	.275	.250
.325	.350	.325	.350	.325	.350
.425	.450	.425	.450	.425	.450
.475	.550	.475	.550	.475	.550
.525	.625	.525	.625	.525	.625
.625	.675	.625	.675	.625	.675
.675	.750	.675	.750	.675	.750
.750	.850	.750	.850	.750	.850
.850	.950	.850	.950	.850	.950
.950	-----	.950	-----	.950	-----
Station 4		Station 5		Station 6	
0	-----	0	-----	0	-----
.004	-----	.0018	-----	.0074	-----
.0053	-----	.0051	-----	------	-----
.013	0.013	.013	0.013	.013	0.013
.038	.038	.038	.038	.038	.038
.063	.063	.063	.063	.063	.063
.125	.088	.125	.088	.125	.088
.175	.125	.175	.125	.175	.125
.225	.175	.225	.175	.225	.175
.275	.250	.275	.250	.275	.250
.325	.350	.325	.350	.325	.350
.425	.450	.425	.450	.425	.450
.475	.550	.475	.550	.475	.550
.575	.625	.575	.625	.575	.625
.625	.675	.625	.675	.625	.675
.675	.750	.675	.750	.675	.750
.750	.850	.750	.850	.750	.850
.850	.950	.850	.950	.850	.950
.950	-----	.950	-----	.950	-----

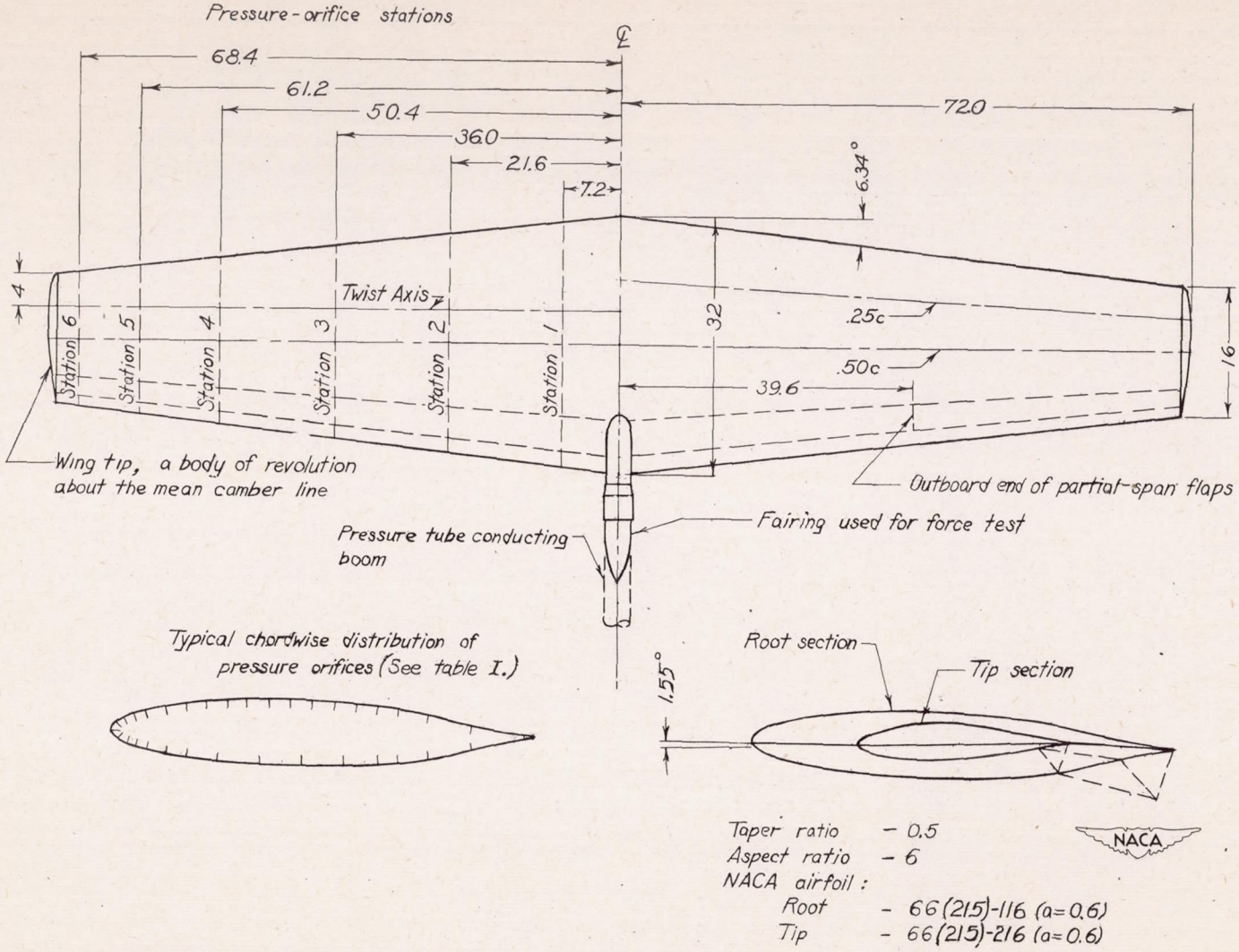

Figure 1.- Layout of wing of NACA 66-series airfoil sections. (All dimensions in inches.)

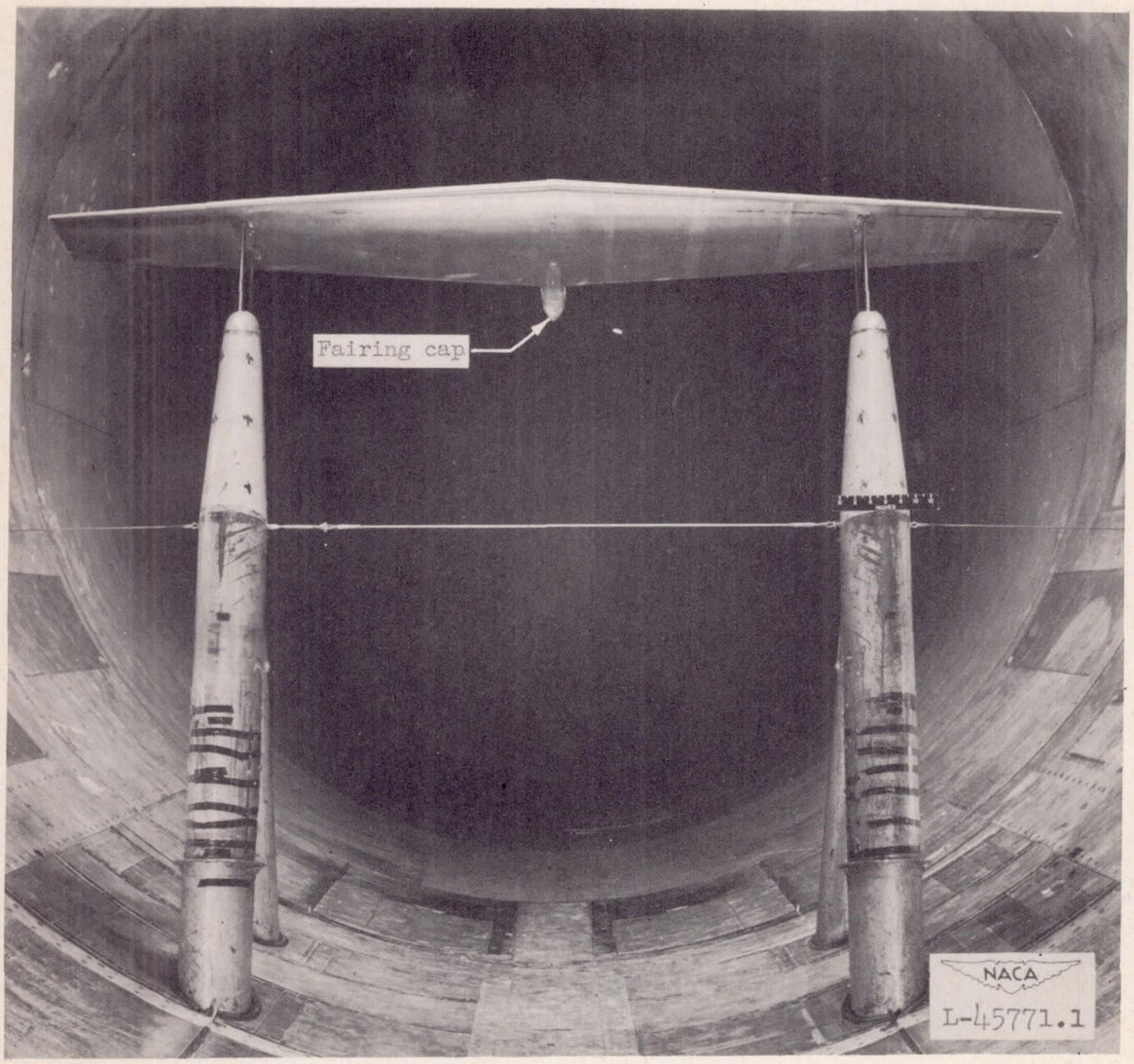

Figure 2.- Wing of NACA 66-series airfoil sections mounted in the Langley 19-foot pressure tunnel.

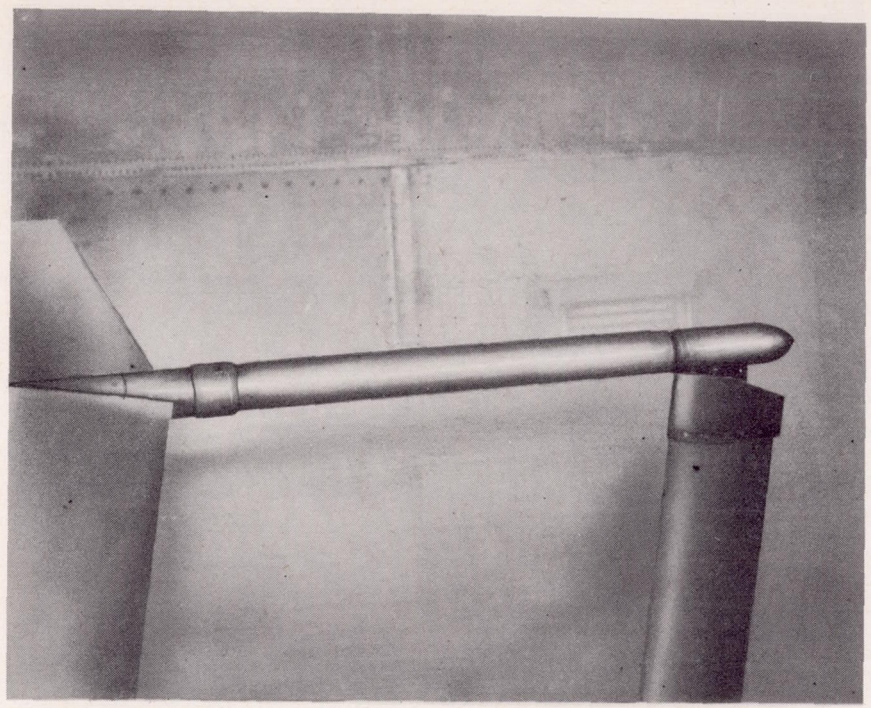

Figure 3.- Close-up of tube-transfer system used in tests of a wing of NACA 66-series airfoil sections in the Langley 19-foot pressure tunnel.

L-45976.1

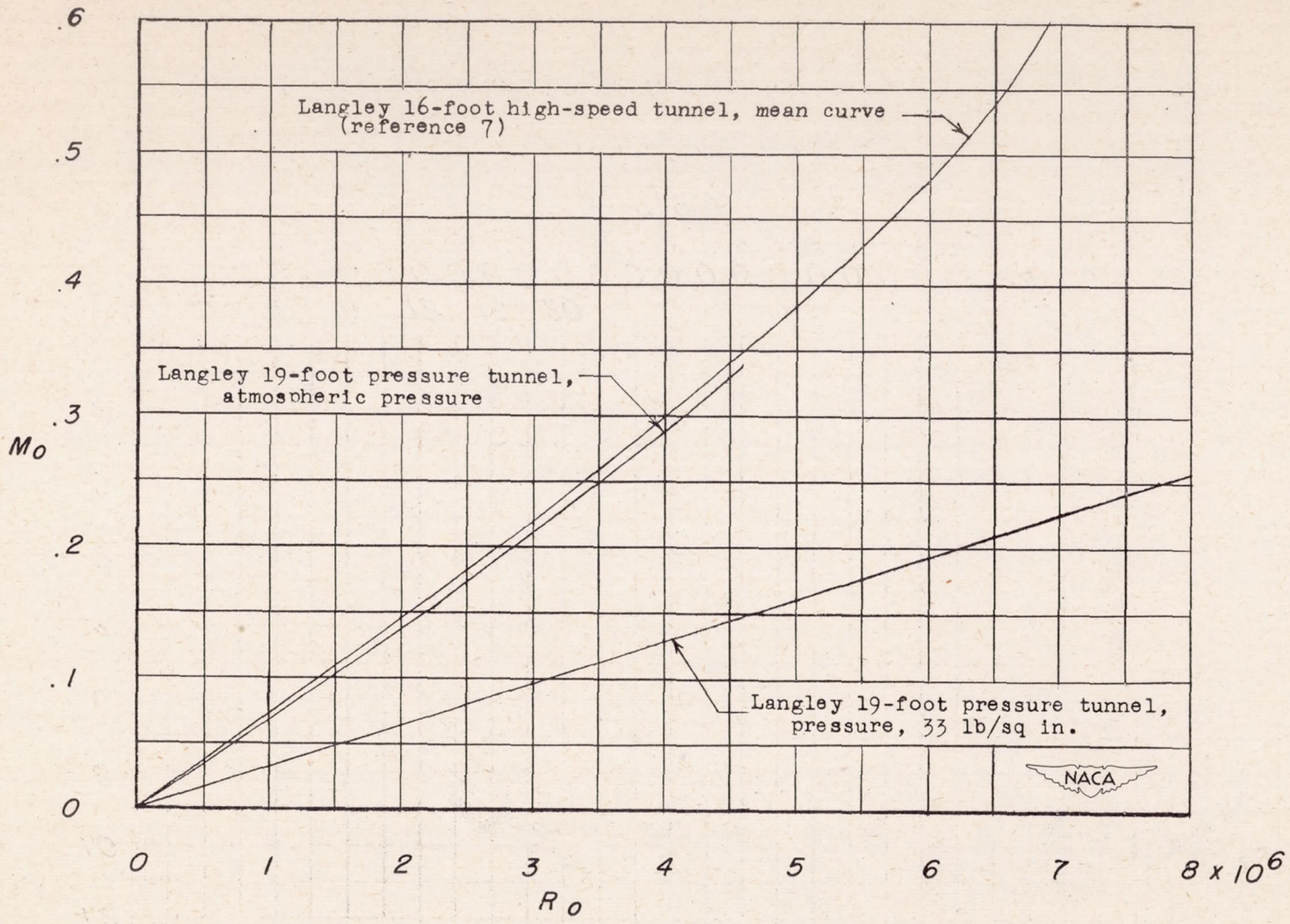

Figure 4.- Test conditions for the wing of NACA 66-series airfoil section in Langley 19-foot pressure tunnel and Langley 16-foot high-speed tunnel.

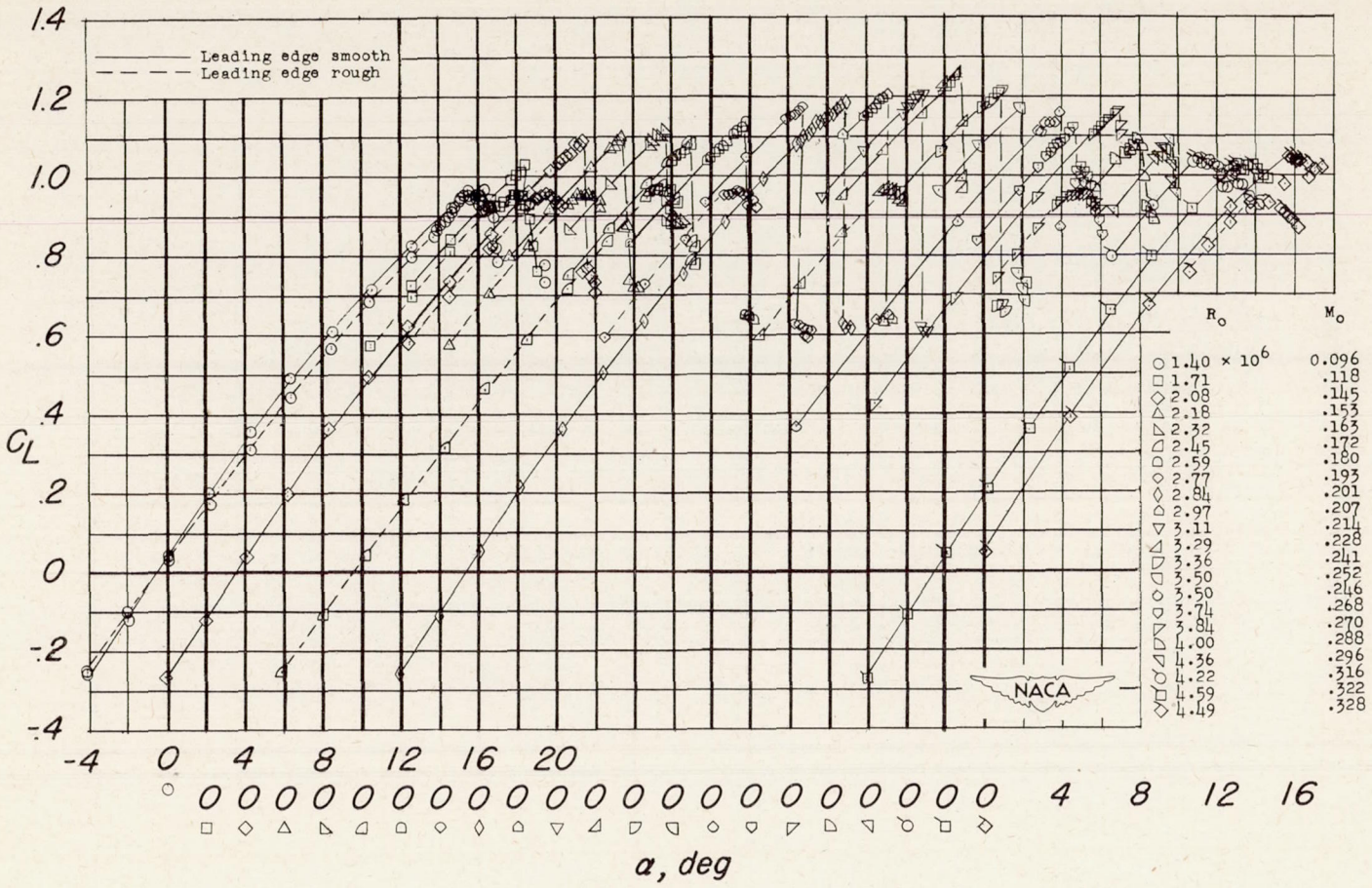

(a) Atmospheric pressure.

Figure 5.- Variation of lift coefficient with angle of attack; plain wing.

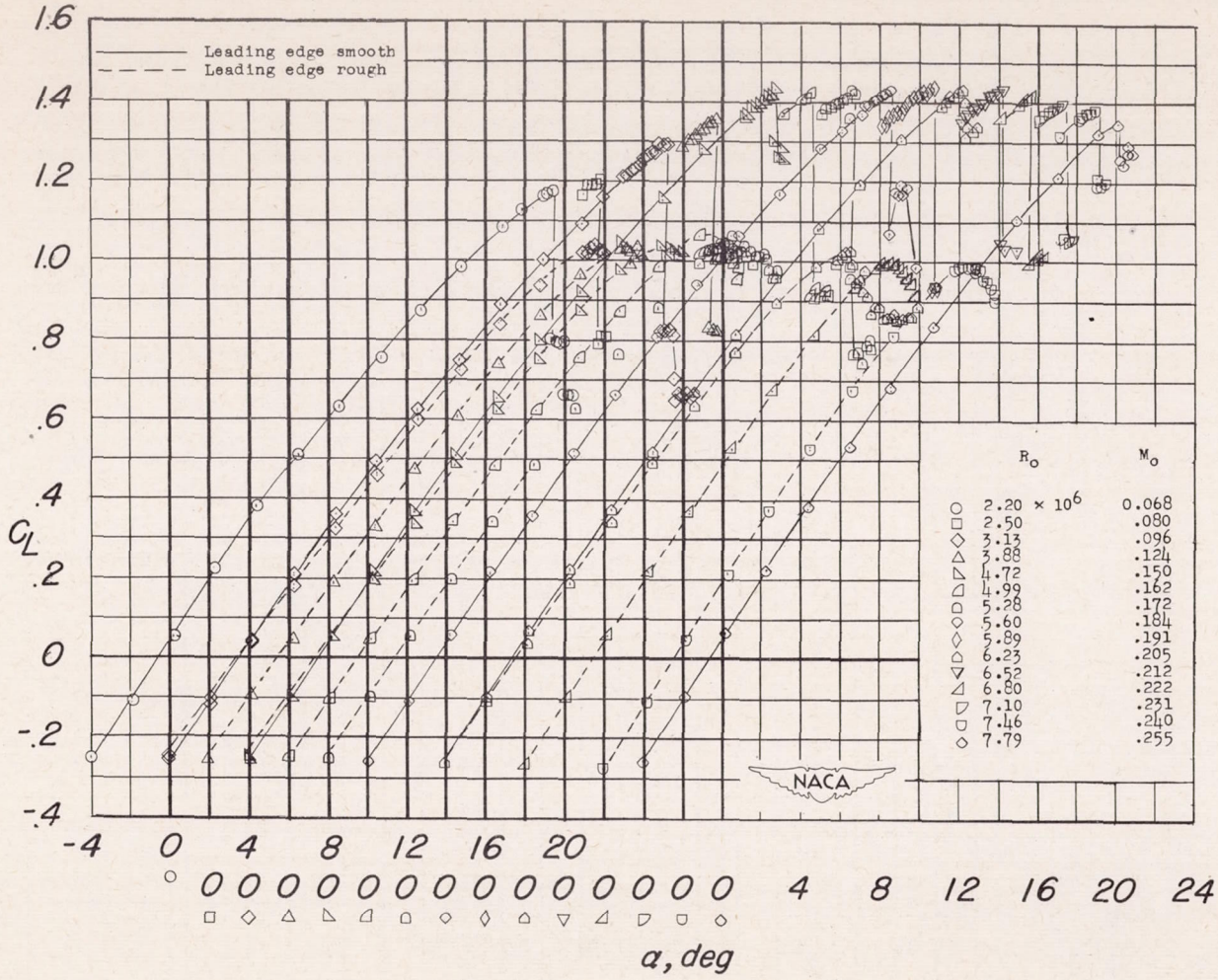

(b) Pressure, 33 pounds per square inch.

Figure 5.- Concluded.

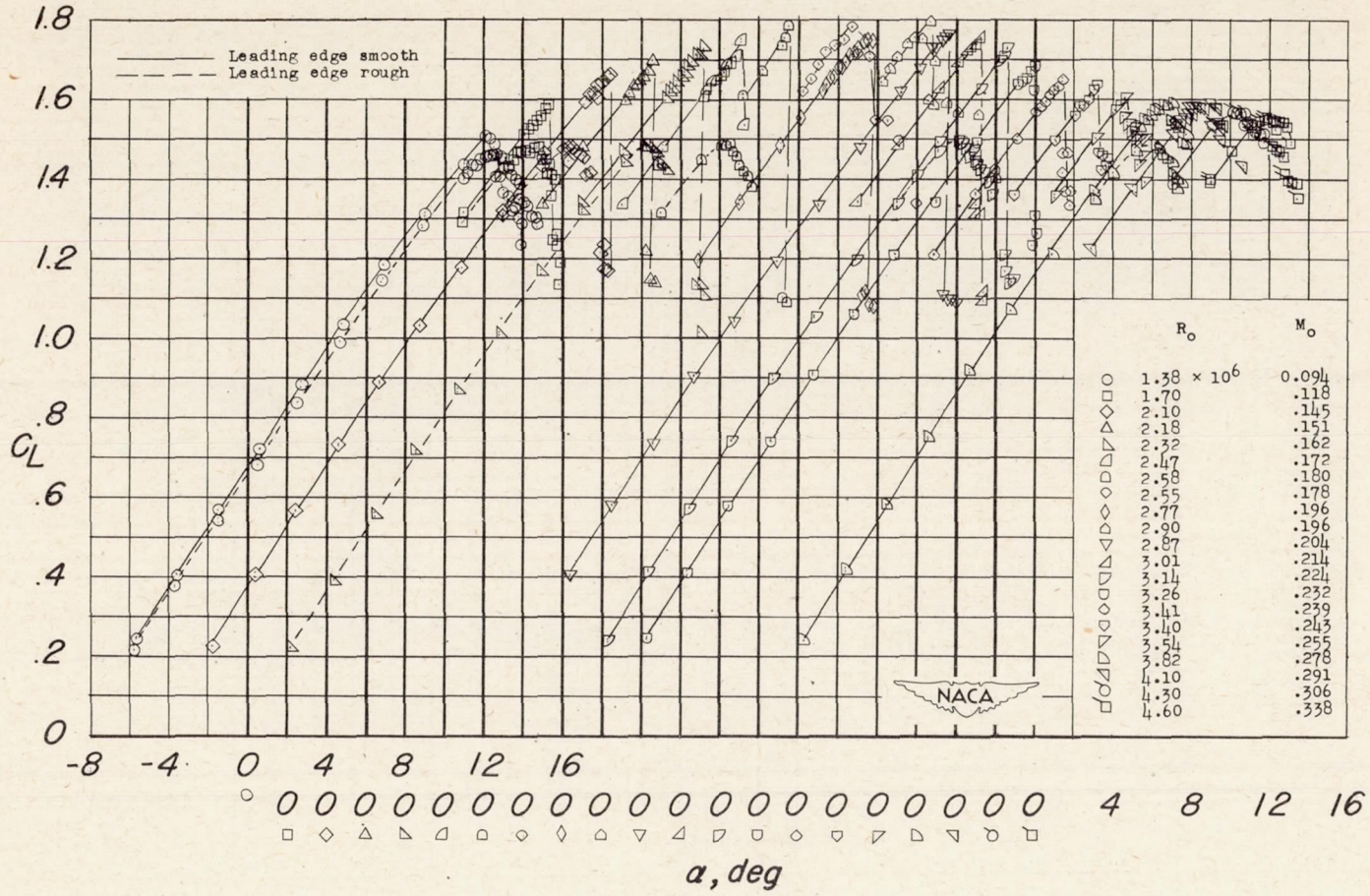

(a) Atmospheric pressure.

Figure 6.- Variation of lift coefficient with angle of attack; partial-span flap configuration.

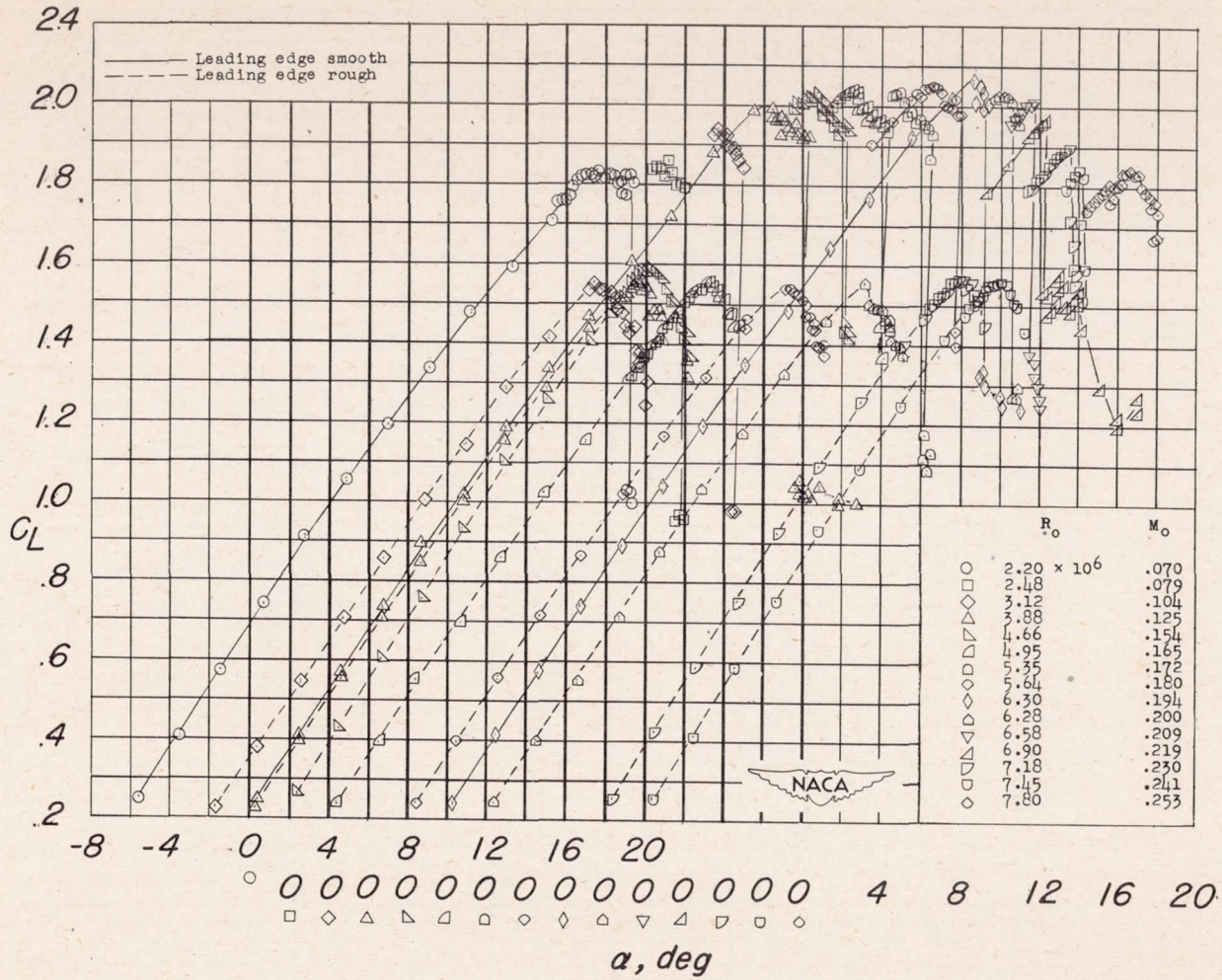

(b) Pressure, 33 pounds per square inch.

Figure 6.- Concluded.

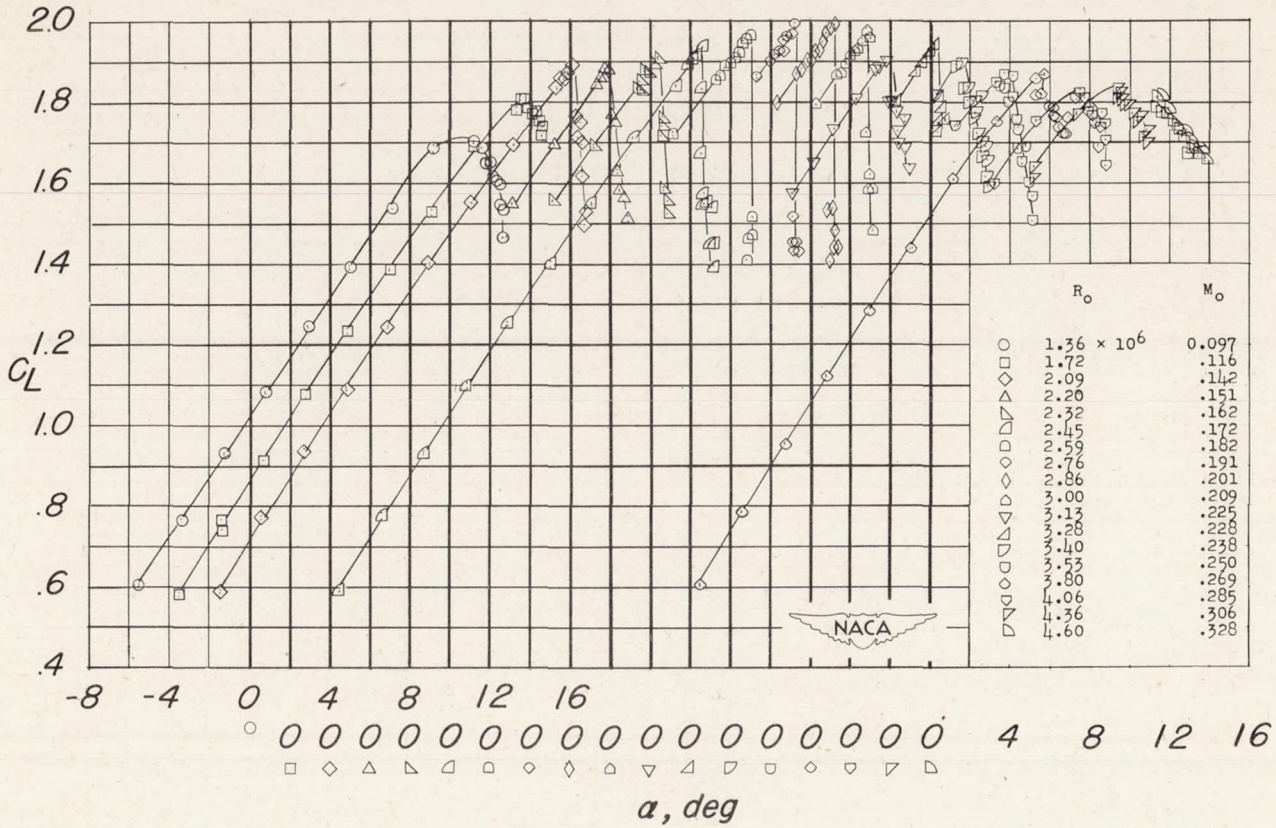

(a) Atmospheric pressure.

Figure 7.- Variation of lift coefficient with angle of attack; full-span flap configuration.

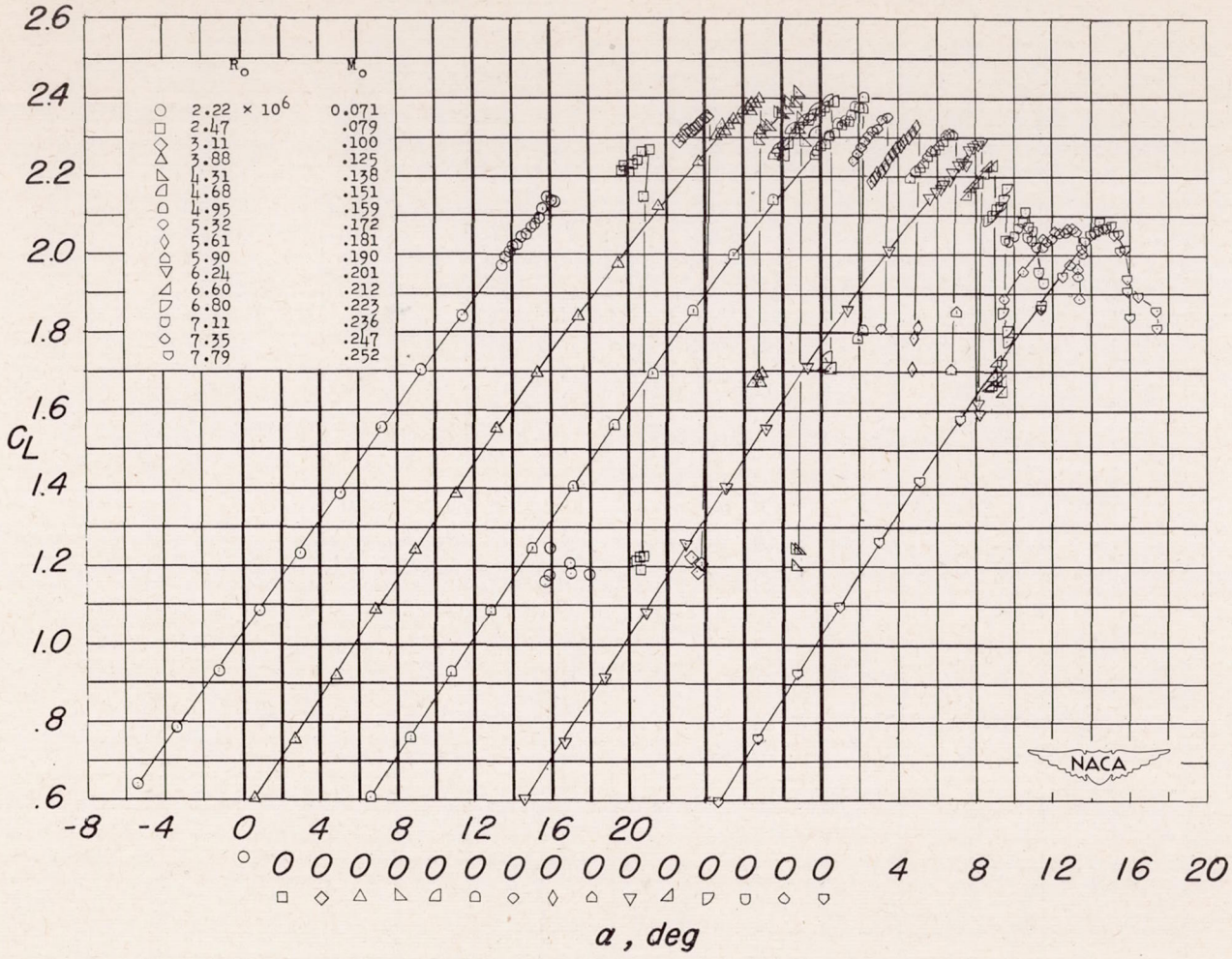

(b) Pressure, 33 pounds per square inch.

Figure 7.- Concluded.

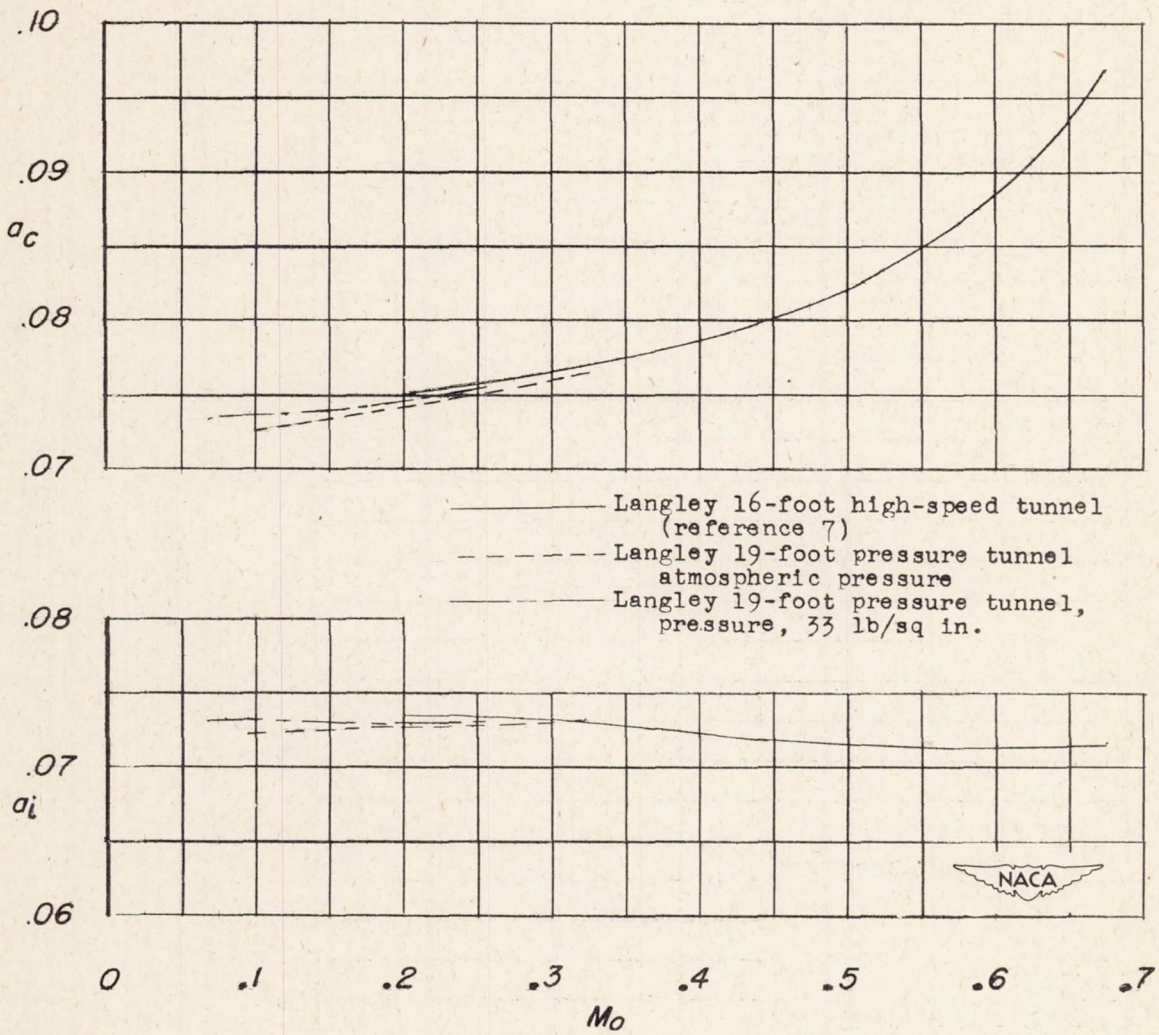

Figure 8.- Variation of lift-curve slopes with Mach number.

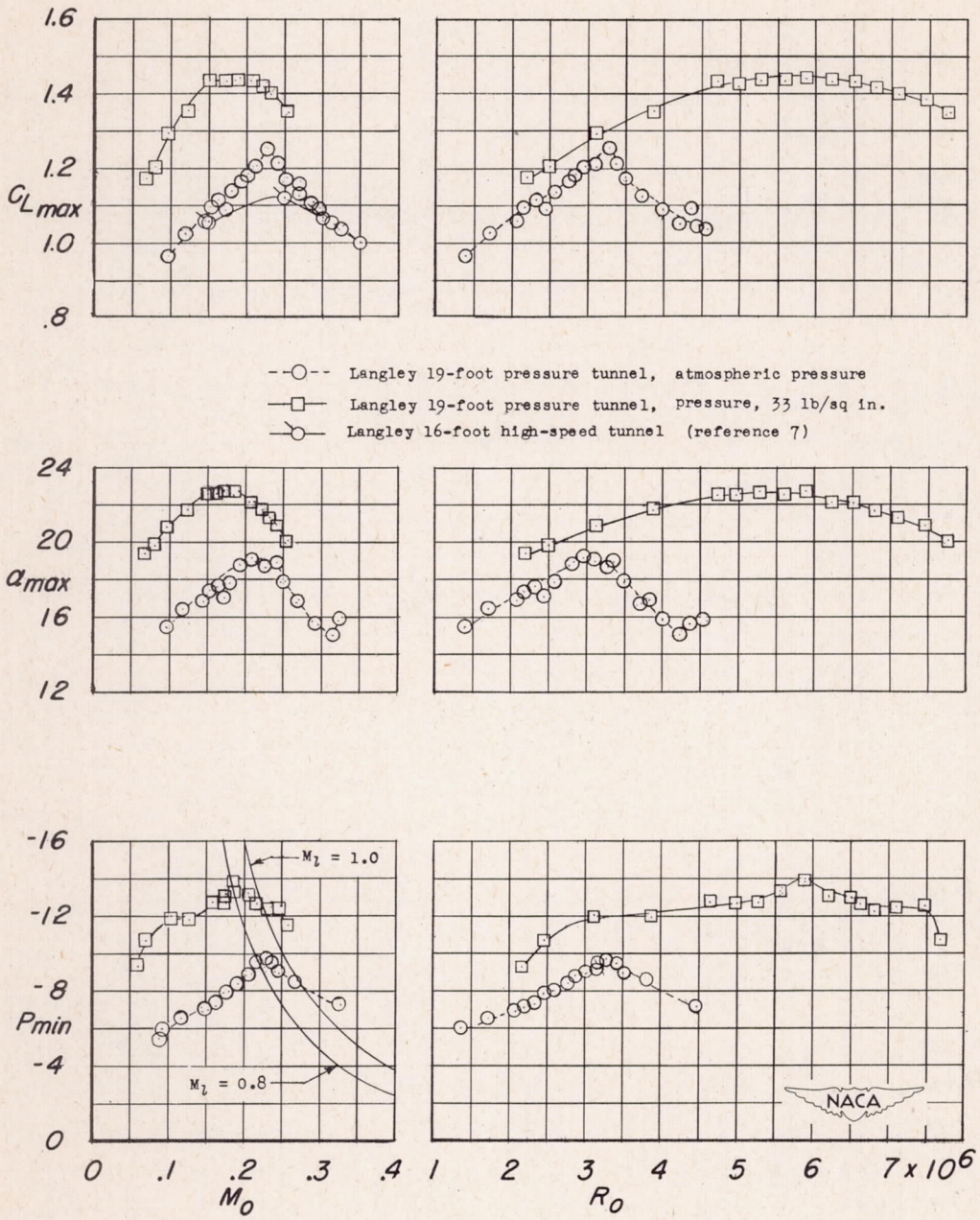

(a) Plain wing.

Figure 9.- Variation of the maximum lift coefficient, angle of attack for maximum lift coefficient, and minimum pressure coefficient with Mach number and Reynolds number.

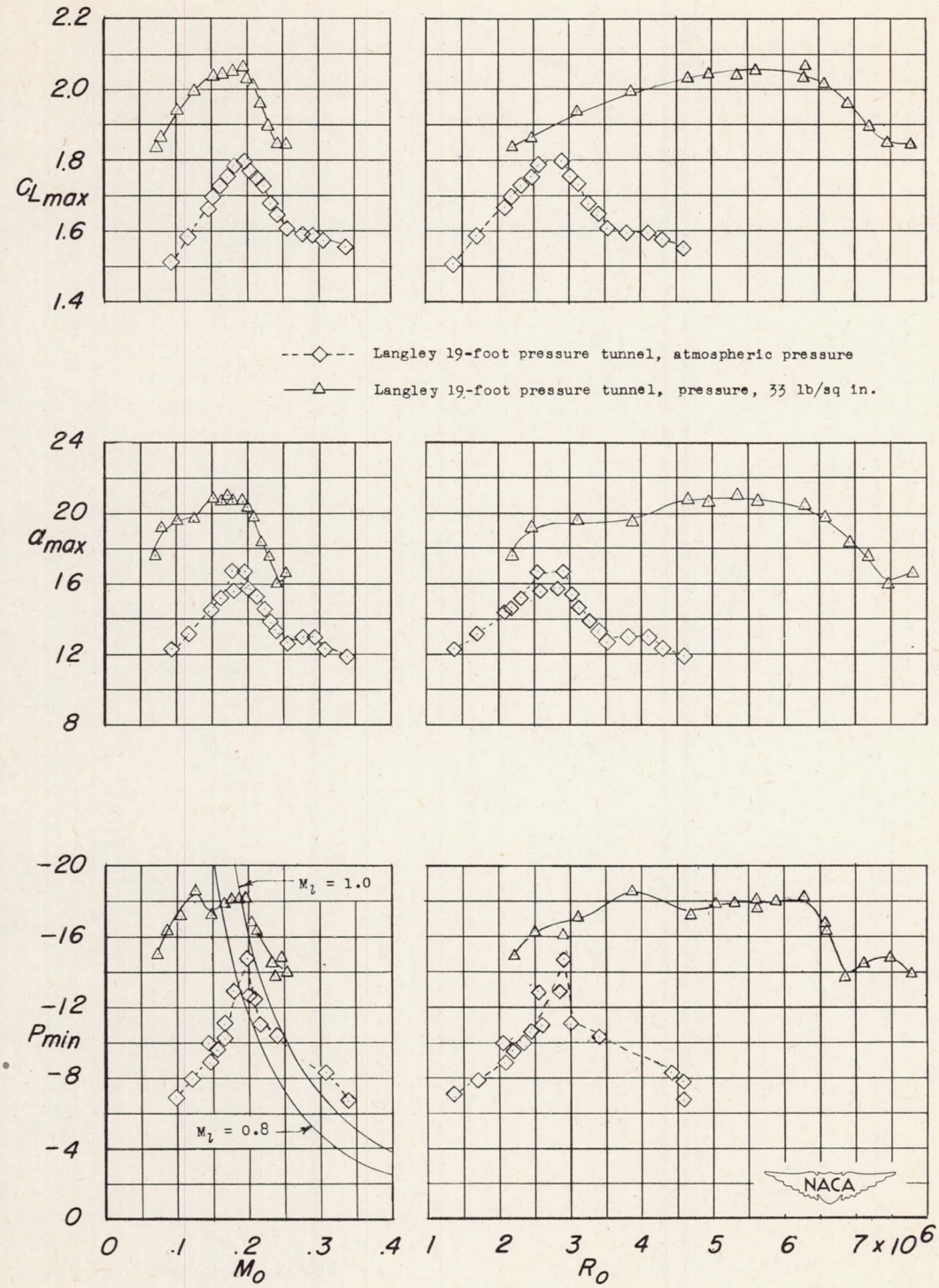

(b) Partial-span flap configuration.

Figure 9.- Continued.

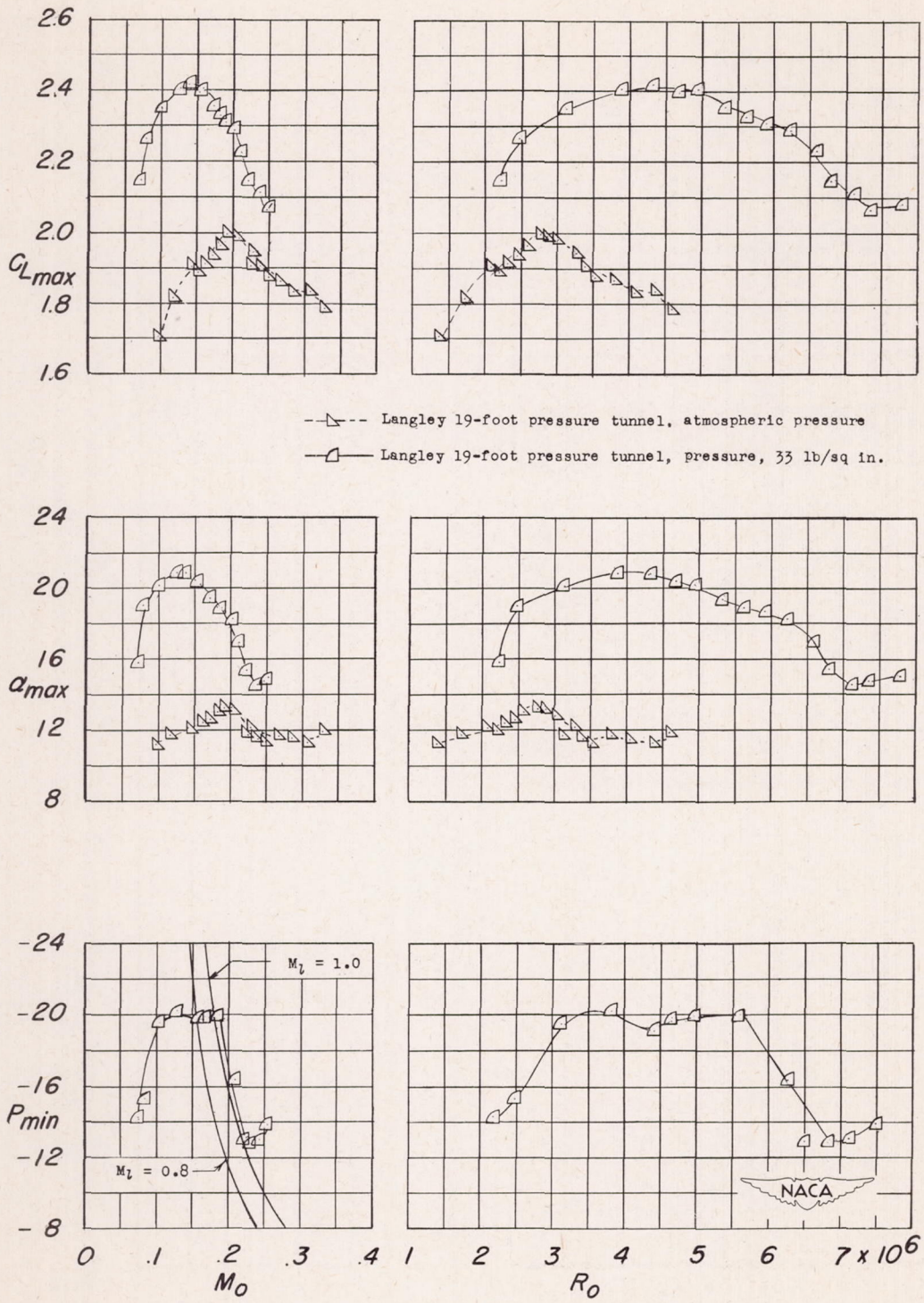

(c) Full-span flap configuration.

Figure 9.- Concluded.

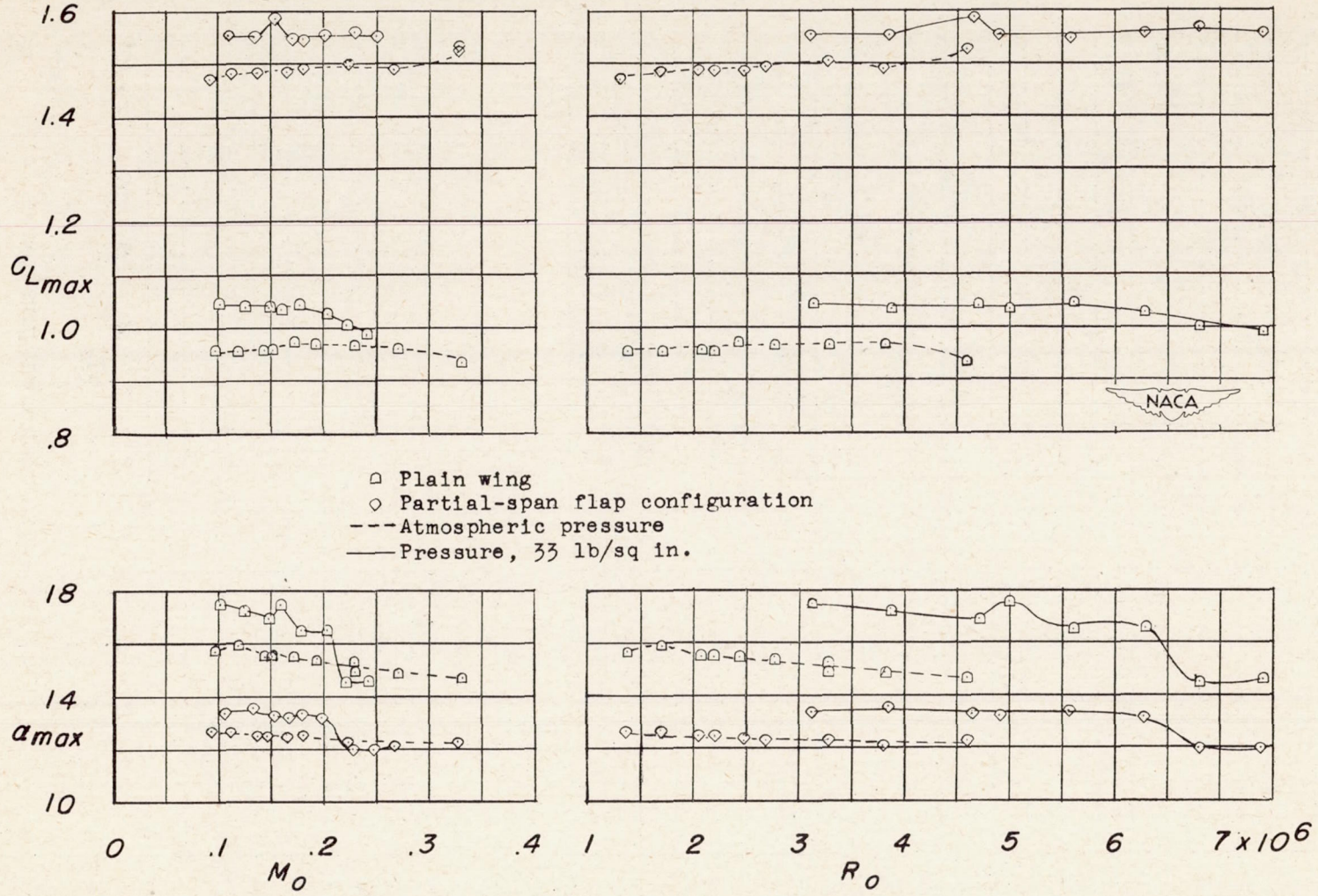

Figure 10.- Variation of maximum lift coefficient and angle of attack for maximum lift coefficient with Mach number and Reynolds number. Leading edge rough.

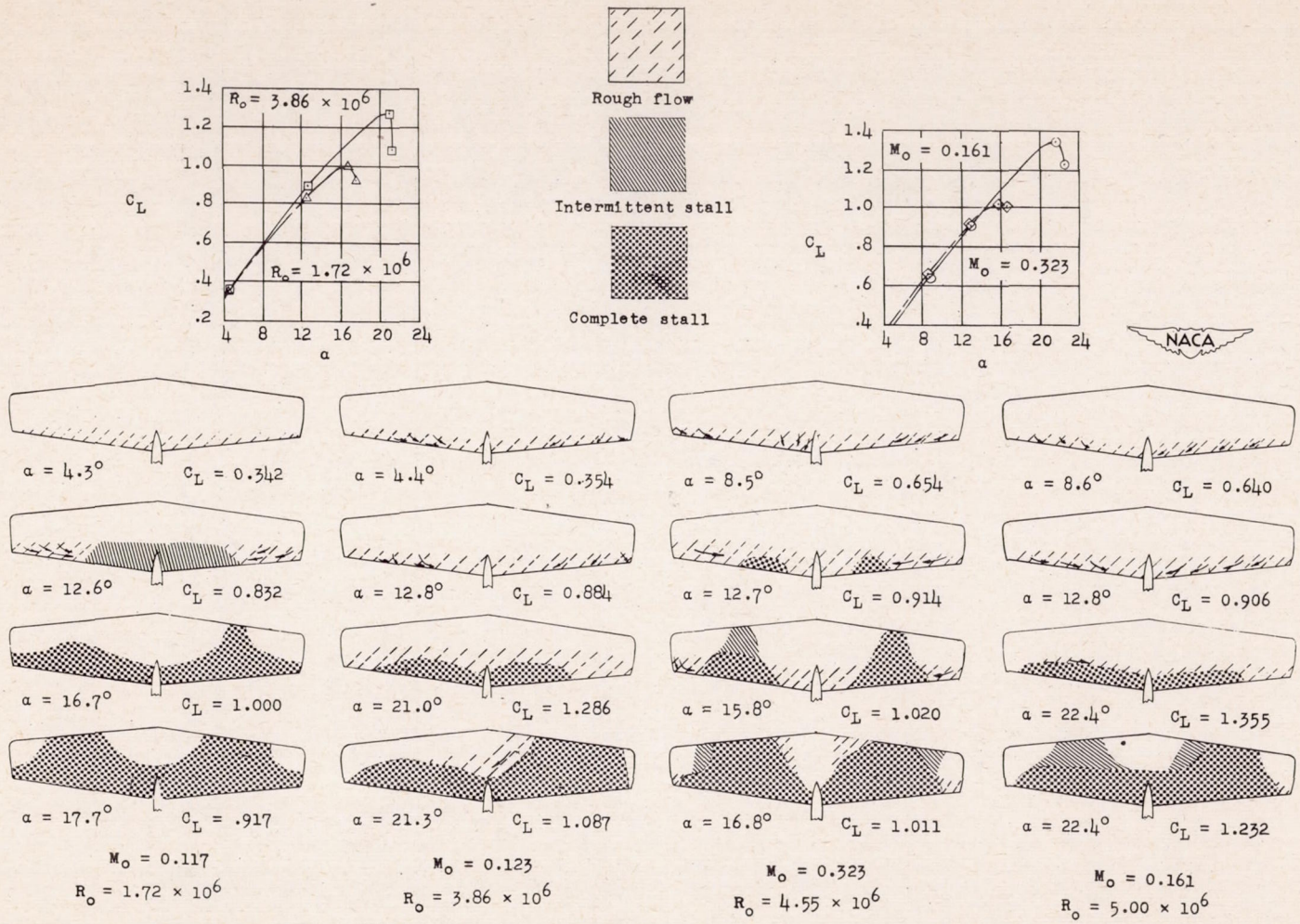

(a) Effects of R_o; M_o approximately constant. (b) Effects of M_o; R_o approximately constant.

Figure 11.- Comparison of stalling patterns at various Mach numbers and Reynolds numbers. Plain wing.

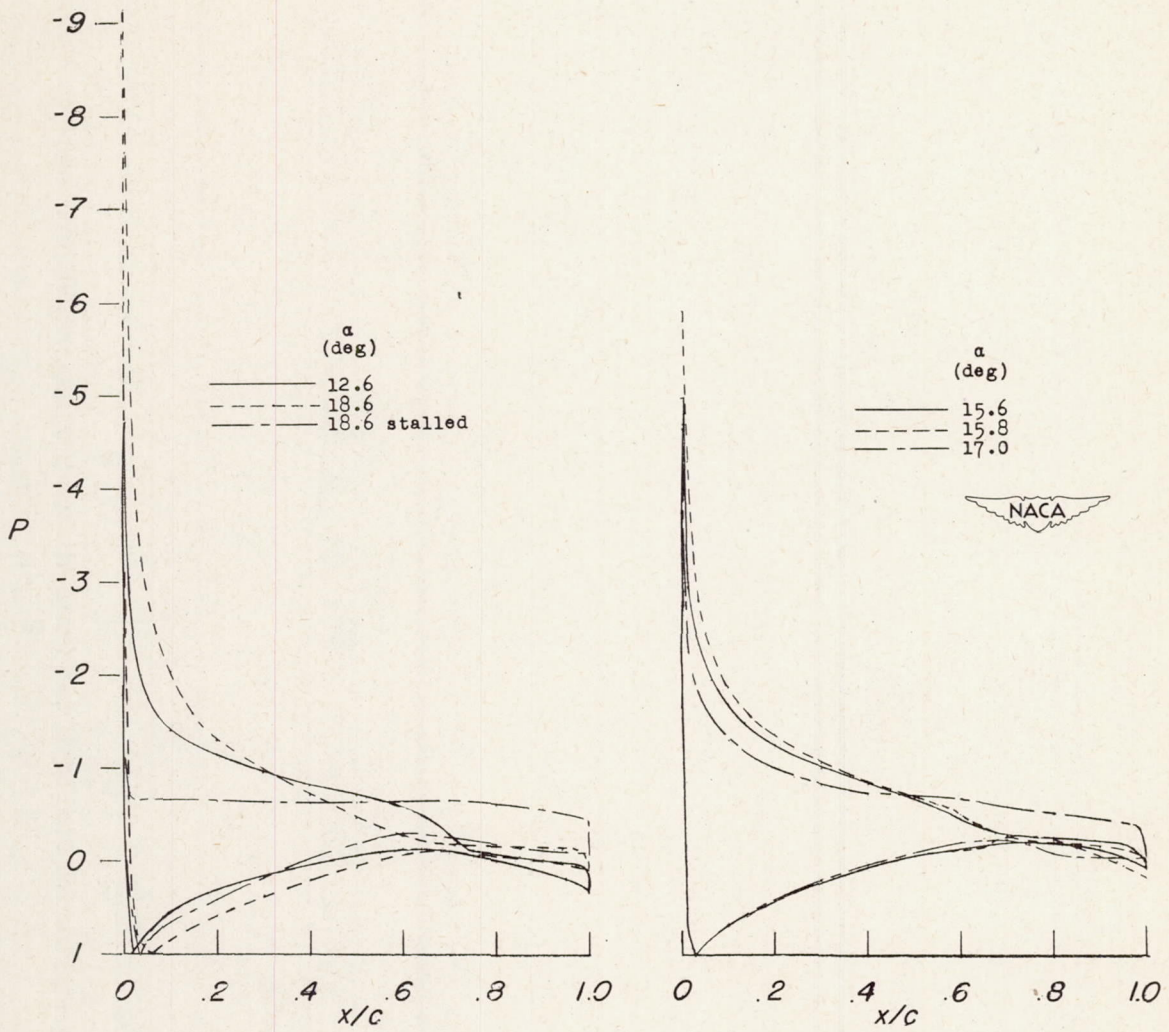

(a) $M_o = 0.228$; $R_o = 3.29 \times 10^6$. (b) $M_o = 0.328$; $R_o = 4.29 \times 10^6$.

Figure 12.- Typical chordwise pressure distribution showing the amount of separation below and above the critical Mach number on the plain wing.

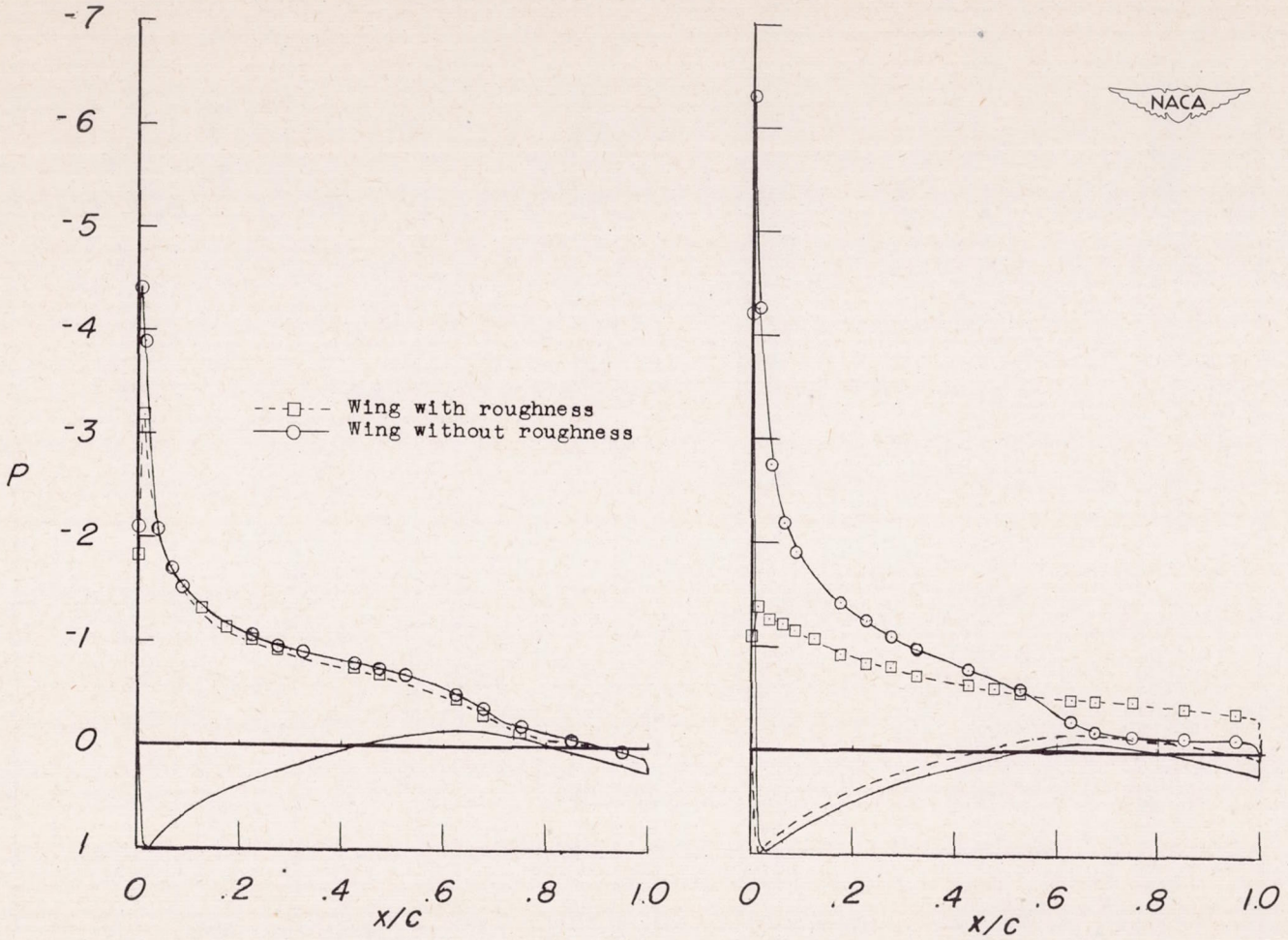

(a) $\alpha = 12.6^{\circ}$.

(b) $\alpha = 16.7^{\circ}$.

Figure 13.- Comparison of chordwise pressure distribution with and without leading-edge roughness. $M_o = 0.220$; $R_o = 3.26 \times 10^6$.

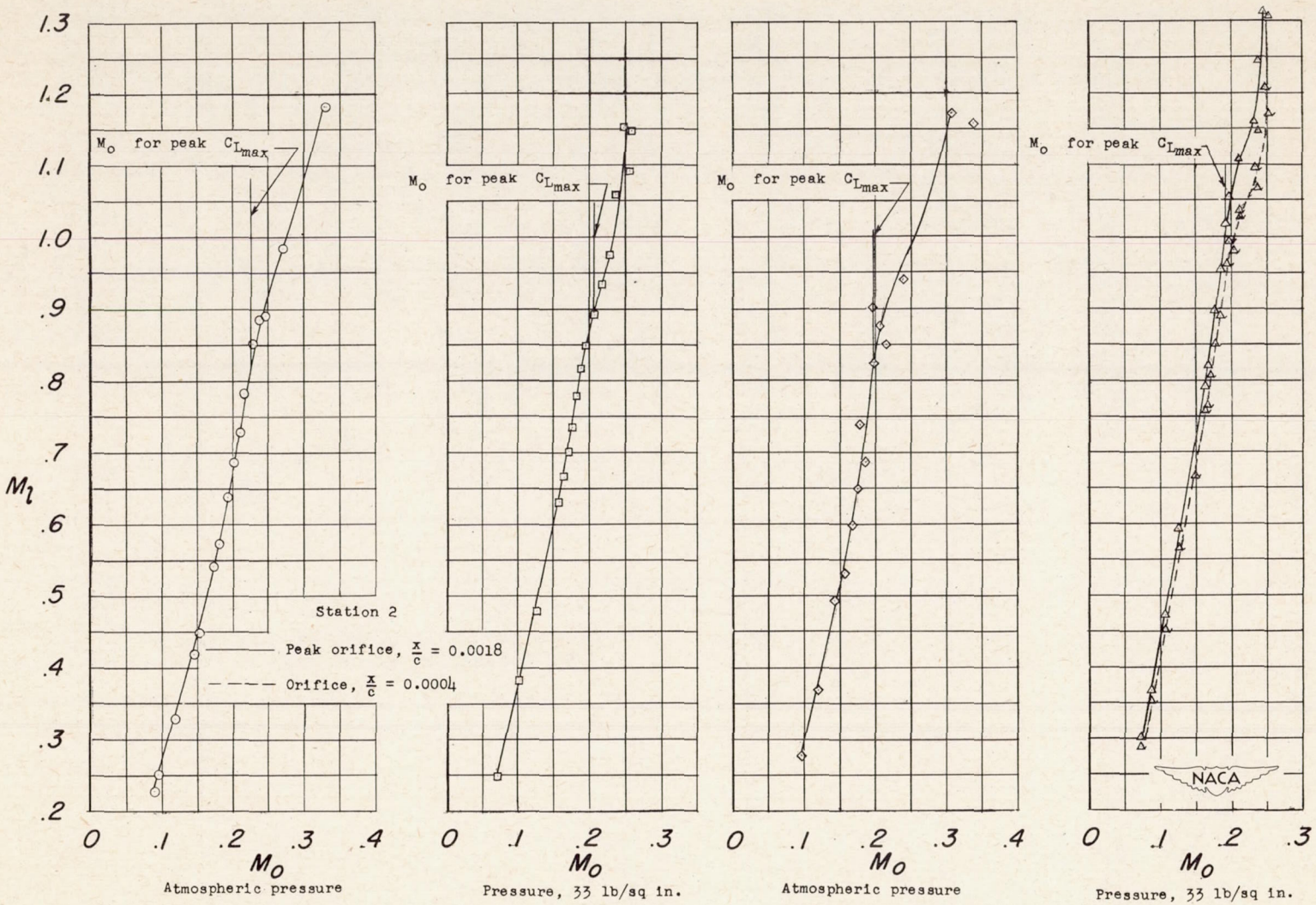

(a) Plain wing. (b) Partial-span flaps.

Figure 14.- Variation of local Mach number with free-stream Mach number.

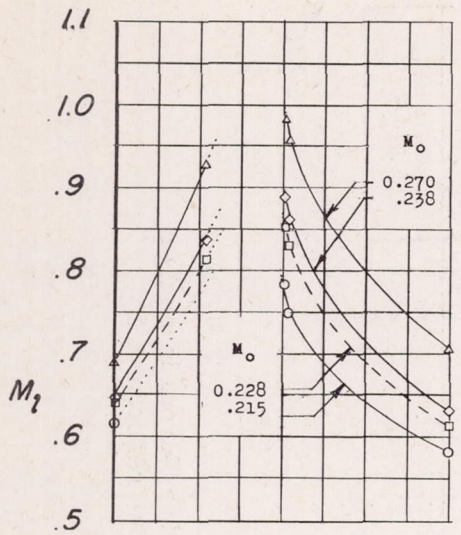

(a) Plain wing; atmospheric pressure.

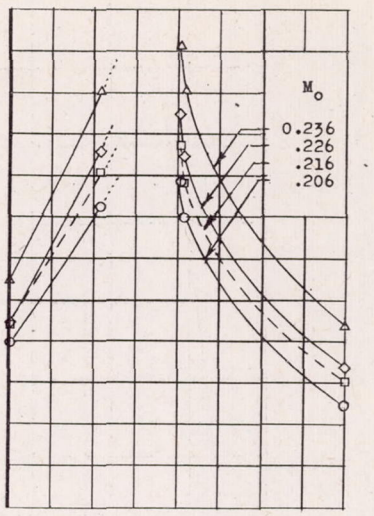

(b) Plain wing, pressure, 33 pounds per square inch.

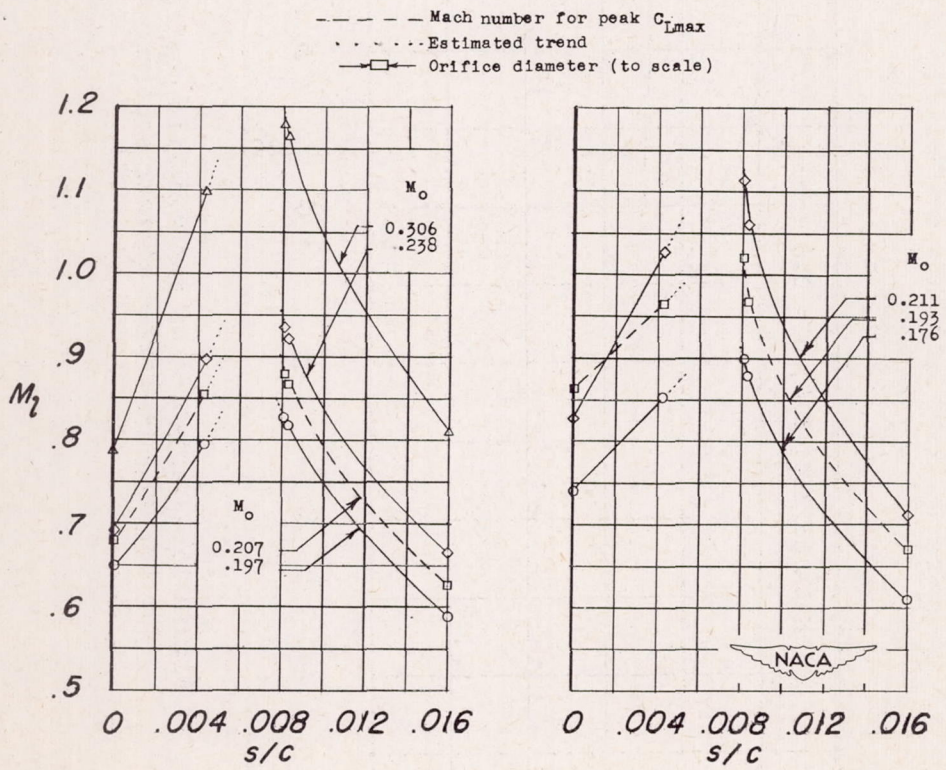

(c) Partial-span flaps; atmospheric pressure.

(d) Partial-span flaps; pressure, 33 pounds per square inch.

Figure 15.- Variation of local Mach number with distance from the leading edge. Data obtained at station 2.

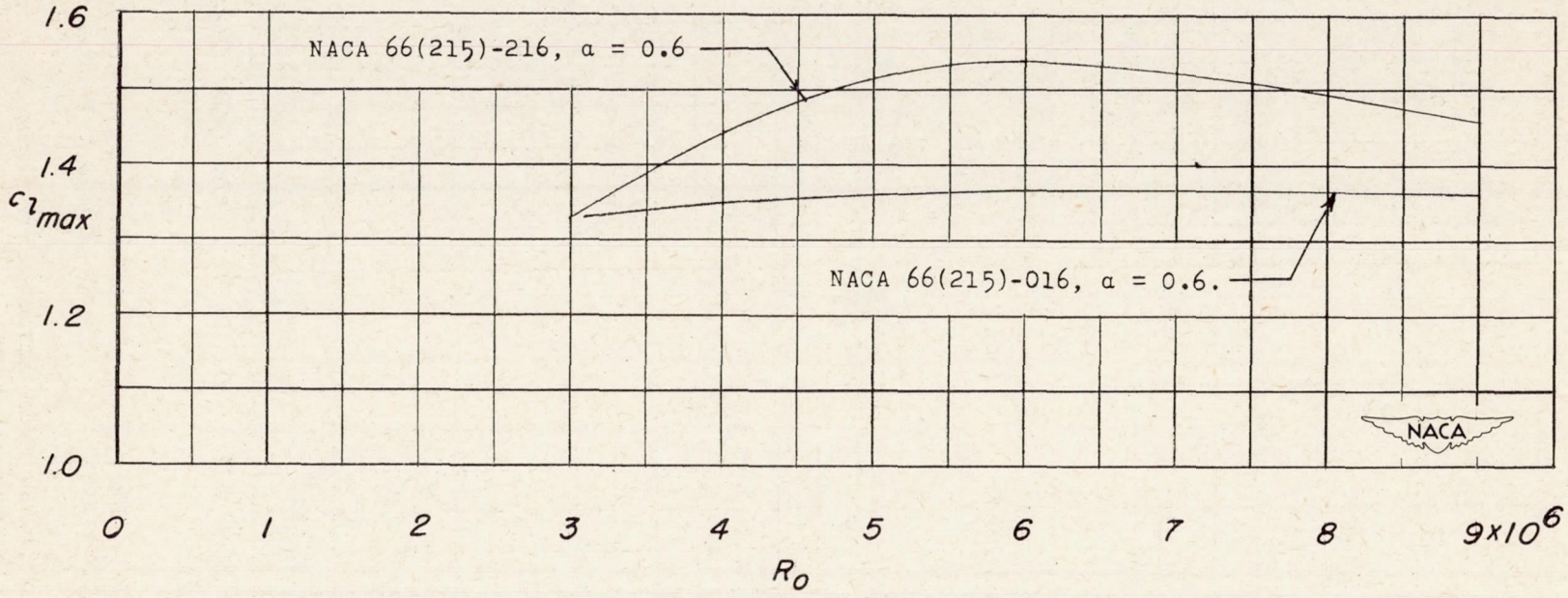

Figure 16.- Variation of maximum lift coefficient with Reynolds number for two NACA 66-series airfoil sections (data from reference 15).

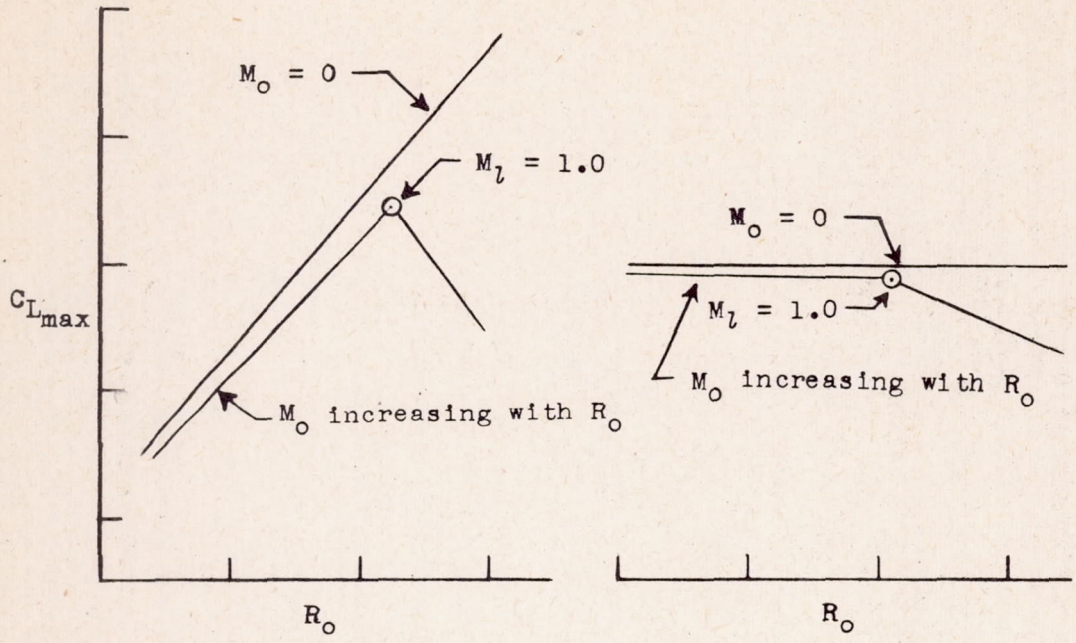

(a) Case I. (b) Case II.

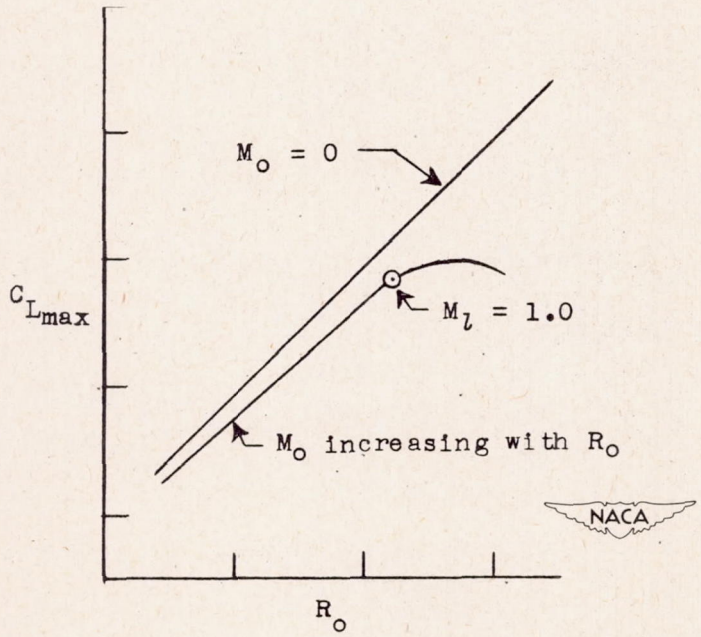

(c) Case III.

Figure 17.- Schematic curves illustrating the effect of varying M_o with R_o on the maximum lift-coefficient variation with R_o for several types of wings.